

THE ACID/BASE PROPERTIES OF 1-ADAMANTANAMINE IN  
AQUEOUS-ACETONITRILE SOLUTIONS STUDIED BY FOURIER  
TRANSFORM INFRARED SPECTROMETRY

by

Roseann Theresa Baca

Submitted in Partial Fulfillment of the Requirements  
for the Degree of  
Master of Science  
in the  
Chemistry  
Program

Daryl W. Murray 8-25-87  
Adviser Date

Sally M. Hotchkiss August 27, 1987  
Dean of the Graduate School Date

YOUNGSTOWN STATE UNIVERSITY

August, 1987

187

188

189  
1-01-1

190

191

YOUNGSTOWN STATE UNIVERSITY

Graduate School

THESIS

Submitted in Partial Fulfillment of the Requirements  
For the Degree of MASTER OF SCIENCE

TITLE: THE ACID/BASE PROPERTIES OF 1-ADAMANTANAMINE  
IN AQUEOUS-ACETONITRILE SOLUTIONS STUDIED  
BY FOURIER TRANSFORM INFRARED SPECTROMETRY

PRESENTED BY Roseann Theresa Baca

ACCEPTED BY THE DEPARTMENT OF CHEMISTRY

Rayl W. Mincey 8-25-87  
Major Professor Date

Kenneth S. Routhal 8-24-87

Thomas Dobbstein 8-25-87

Sally M. Hatcher 8-27-87  
Dean, Graduate School Date

By the way, I'm

going to be

going to be

going to be

going to be

going to be

going to be

going to be

going to be

going to be

going to be

going to be

going to be

going to be

## ABSTRACT

The **Acid/Base** Properties of **1-Adamantanamine** in Aqueous  
Acetonitrile Solutions Studied by  
Fourier Transform Infrared Spectrometry

Roseann Theresa Baca

Master of Science

Fourier Transform Infrared Spectroscopy is an instrumental technique which is used for the identification and characterization of chemical compounds. Using this technique, all the frequencies of a broad region of infrared energy can be measured simultaneously. In the past, this technique was not useful in the measurement of aqueous solutions due to the strong O-H absorption bands. This problem has been overcome with the advent of cylindrical internal reflectance techniques.

With these concepts in mind, the decision was made to analyze the characteristics of **1-adamantanamine**, an anti-viral agent, in aqueous-acetonitrile solutions. The effect of varying solvent and pH was studied by comparing and contrasting the infrared spectra of aqueous, 25% acetonitrile, 50% acetonitrile, and 75% acetonitrile solutions of 0.013 M **1-adamantanamine** at pH from 5-13. Two common absorption bands were noted as the solvents and pH **changed**. The absorbance changes of these two peaks at various pH values were then used to calculate the  $pK_a$  value of **1-adamantanamine** in aqueous and mixed solvents.

This  $pK_a$  study was performed with aqueous and mixed solvent solutions of varying hydrophobicity to investigate potential changes in  $pK_a$  of this antiviral agent. The  $pK_a$  value of **1-adamantanamine** in water



was experimentally calculated to be 10.8 and 10.4 for the two peaks, peak A and B, in the infrared spectra of this compound which were monitored. Addition of acetonitrile to 25% of the solvent volume increased the  $pK_a$  determined from Peak A and B to 11.0 and 10.7, respectively. But, further increases in acetonitrile concentration decreased the  $pK_a$  values. It can be concluded that as the hydrophobicity of the solutions increased with increasing acetonitrile concentrations, the  $pK_a$  of the drug remained in the alkaline pH range of 9.7 - 11.0.





#### ACKNOWLEDGEMENTS

I extend my sincerest appreciation to Dr. Daryl Mincey, Dr. Kenneth Rosenthal and Dr. Thomas Dobbelstein for their guidance throughout this research project. In addition, I thank my family and friends for their understanding and support during this project.



TABLE OF CONTENTS

	Page
Abstract.....	ii
Acknowledgements.....	iv
Table of Contents.....	v
List of Symbols.....	viii
List of Figures.....	x
List of Tables.....	xii
Chapter	
I. Introduction: 1-ADAMANTANAMINE,.....	1
Structure and Chemistry.....	1
Pharmacology.....	2
Clinical Uses.....	2
Dosage.....	3
Adverse Reactions.....	3
Contraindications.....	4
Mechanism of Action.....	5
II. HISTORY,.....	6
Principles of Infrared Spectrometry.....	6
Infrared Spectrum of a Substance.....	7
Trends in Infrared Spectrometry.....	9
Theory of Fourier Transform Infrared Spectrometry,...	9
Introduction.....	9
The Michelson Interferometer.....	10
Types of Interferometers.....	13
Sampling the Interferometer.....	13
Computing Techniques.....	14



	Page
Factors Affecting the Interferogram and Spectrum.....	15
Resolution.....	15
Apodization.....	16
Smoothing.....	17
Baseline Adjustment.....	17
Spectral Subtraction and Addition.....	18
Fourier Transform Infrared Spectrometers	
Instrumental Design.....	18
Interferometer Design and Drive Systems.....	18
Sources for Fourier Transform Spectrometers.....	21
Infrared Detectors.....	21
Data Systems.....	22
Sampling Techniques - Cylindrical Internal Reflection.....	23
Advantages of Fourier Transform Infrared Spectrometry.....	25
Disadvantages.....	27
Summary of the Fourier Transform Infrared Spectrometry of Aqueous Solutions.....	28
<b>III. APPARATUS AND MATERIALS.....</b>	<b>31</b>
IR/32 FTIR Spectrometer.....	31
pH Meter.....	34
Combination pH Electrode.....	34
Chemicals.....	36
<b>IV. EXPERIMENTAL METHODS.....</b>	<b>37</b>
Introduction.....	37
Part A: Preparation of Reagents.....	37
Part B: Flow-thru cell and pump set-up.....	38



	Part C: FTIR Measurement of Samples.....	38
	Standard Operating Procedure.....	38
	Collection of Background and Sample.....	41
	Part D: Manipulation of Spectral Data.....	42
V.	EXPERIMENTAL RESULTS AND DISCUSSION .....	43
	Introduction.....	44
	Determination of the pKa values.....	48
VI.	CONCLUSION.....	72
	REFERENCES.....	76





## LIST OF SYMBOLS

SYMBOLS	DEFINITIONS
A or Abs	Absorbance
$A^-$	Alkaline form
$A_a$	Absorbance of HA
$A_b$	Absorbance of $A^-$
cm	Centimeter
$cm^{-1}$	Reciprocal centimeter
CIR	Cylindrical Internal Reflection
	Fixed mirror
FTIR	Fourier Transform Infrared Spectroscopy
g	Grams
HA	Acid Form
IR	Infrared
Log	Logarithm
	Moveable mirror
MCT	Mercury <b>Cadium</b> Telluride Detector
mg	Milligram
mL	Milliliter
pH'	Measured pH
$pK_a$	Negative logarithm of the dissociation constant
T	Transmittance
[ ]	Molar concentration
$^{\circ}C$	Degrees Celsius



®

Trademark

μm

Micrometers

λ

Wavelength

\*\*

Equilibrium constants calculated  
for mixed solvents



LIST OF FIGURES

Figure	Page
1. Structure of <b>1-Adamantanamine</b> .....	1
2. Types of molecular vibrations.....	8
3. Schematic diagram of Michelson Interferometer.....	11
4. Block diagram of an FTIR analyzer.....	19
5. Optical diagram of a Flow-thru Circle Accessory.....	24
6. Block diagram of the IR/32 main assembly.....	32
7. Schematic diagram of the IR/32 optics bench.....	33
8. Diagram of a Circle Cell Accessory.....	35
9. Diagram of the flow-thru cell and set-up.....	39
10. IR spectrum of <b>1-Adamantanamine</b> in water at pH 11.....	44
11. IR spectrum of <b>1-Adamantanamine</b> in 25% Acetonitrile at pH 11.....	45
12. IR spectrum of <b>1-Adamantanamine</b> in 50% Acetonitrile at pH 11.....	46
13. IR spectrum of <b>1-Admanatanamine</b> in 75% Acetonitrile at pH 11.....	47
14. Typical Plot of absorbance vs pH for a weak acid. HA.....	53-
15. Absorbance vs pH for peak A in water.....	54
16. Absorbance vs pH for peak B in water.....	55
17. Absorbance vs pH for peak A in 25% Acetonitrile.....	56
18. Absorbance vs pH for peak B in 25% Acetonitrile.....	57
19. Absorbance vs pH for peak A in 50% Acetonitrile.....	58
20. Absorbance vs pH for peak B in 50% Acetonitrile.....	59
21. Absorbance vs pH for peak A in 75% Acetonitrile.....	60
22. Absorbance vs pH for peak B in 75% Acetonitrile.....	61
23. Log [A-]/[HA] vs pH for peak A in water.....	63
24. Log [A-]/[HA] vs pH for peak B in water.....	64



25. Log [A-]/[HA] vs pH for peak A in 25% Acetonitrile.....	65
26. Log [A-]/[HA] vs pH for peak B in 25% Acetonitrile.....	66
27. Log [A-]/[HA] vs pH for peak A in 50% Acetonitrile.....	67
28. Log [A-]/[HA] vs pH for peak B in 50% Acetonitrile.....	68
29. Log [A-]/[HA] vs pH for peak A in 75% Acetonitrile.....	69
30. Log [A-]/[HA] vs pH for peak B in 75% Acetonitrile.....	70





## LIST OF TABLES

TABLE	PAGE
1. Instrumental specifications used during this project.....	40
2. Experimental data obtained from Peaks A and B in aqueous solutions.....	49
3. Experimental data obtained from Peaks A and B in 25% acetonitrile solutions.....	50
4. Experimental data obtained from Peaks A and B in 50% acetonitrile solutions.....	51
5. Experimental data obtained from Peaks A and B in 75% acetonitrile solutions.....	52
6. Adjusted $pK_a$ values obtained from Peaks A and B in the various concentrations of acetonitrile.....	71



## CHAPTER I

### INTRODUCTION

#### 1-ADAMANTANAMINE

##### Structure and Chemistry

1-Adamantanamine,  $C_{10}H_{17}N$ , also known as amantadine, 1-aminoadamantane, and Tricyclo (3.3.1.1<sup>3,7</sup>) decan-1-amine is a tricyclic amine. Its structure is illustrated in Figure 1. Other pertinent physical and chemical data for this compound include: a melting point of 206-208 °C, a molecular weight of 151.25 g, and its action as a lysosomotropic weak base.<sup>1,2,3,4</sup>

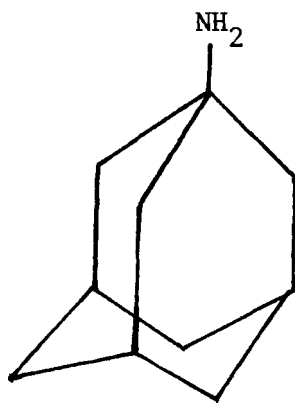


Figure 1 - Structure of 1-adamantanamine<sup>3</sup>

The hydrochloride form, 1-adamantanamine hydrochloride, is a white, crystalline compound which is soluble in both water and alcohol.<sup>5</sup> As Symmetrel ®, it is used most often as an antiviral agent in the



prophylaxis and symptomatic management of respiratory infections due to the influenza A virus.<sup>6</sup>

### Pharmacology

Pharmacodynamic studies of the absorption, distribution, and excretion of **1-adamantanamine** have demonstrated that the compound is rapidly and completely absorbed from the gastrointestinal tract after oral administration. Peak blood levels are achieved within two to four hours, and the drug's half-life in serum is approximately twenty hours. Approximately ninety percent of the drug is excreted by the kidneys as the unmodified compound. Also, it is excreted relatively slowly, therefore doses taken once or twice a day will maintain blood levels.<sup>7,8,9</sup>

### Clinical Uses

Even though **1-adamantanamine** inhibits the replication of several viruses in vitro, its main application in clinical practice is for the prophylaxis and symptomatic treatment of influenza A infections. This antiviral activity against the influenza A virus was first demonstrated in 1964. Since then, it has been found to be effective against all strains of influenza A tested, including the Texas ( $H_3N_2$ ) and USSR ( $H_1N_1$ ) subtypes.<sup>5,7,10</sup>

Studies have demonstrated that the drug is seventy percent effective as a prophylactic and may also be used as a therapeutic agent against influenza A.<sup>7</sup> One such investigation by O'Donoghue, studied the effect of 100 mg of **1-adamantanamine** on hospitalized patients against Hong Kong influenza A. He found that the drug prevented clinical influenza and decreased the total number of days of hospitalization in patients admitted during an epidemic<sup>9</sup>.



The Center for Disease Control has proposed guidelines for the uses of **1-adamantanamine** described previously, These recommendations are as follows:<sup>11</sup>

1. The drug should be given as quickly as possible after recognition of an influenza outbreak.
2. The drug should be administered to immunodeficient people, to reduce the spread of the virus and maintain care for high risk persons in the home setting, as an adjunct to late **immunization** of high risk individuals, and in individuals for whom the influenza vaccine is contraindicated.
3. When the drug is used as a therapy in high risk groups, it should be administered one to two days after the onset of the illness and continued for two days after the symptoms subside.

#### Dosage

The adult dosage of **1-adamantanamine** hydrochloride is 200 mg daily, either as a single dosage or two equally-divided ones. The drug is available in the form of capsules or syrup. This therapy is maintained for at least 10 days following a known exposure or throughout the six-week risk period.<sup>7</sup>

#### Adverse Reactions

The most common adverse reactions include nausea, anorexia, vomiting, hyperexcitability, tremors, slurred speech, ataxia, psychotic depression, insomnia, lethargy, dizziness, blurred vision, and skin rashes.<sup>12</sup> These side effects appear to be dose related occurring after doses of 300-400 **mg/day** in adults.<sup>8</sup>





## Contraindications

This drug should be administered with caution in patients with impaired liver and kidney function, epilepsy or psychiatric disorders, in pregnancy, or in nursing mothers. Also, the drug should not be administered to children under fifteen years of age who have been exposed to rubella.<sup>8</sup>

## Mechanism of Action

As mentioned previously, **1-adamantanamine** is a synthetic antiviral agent. It is thought to prevent virus replication by impairing the attachment and penetration of the virus into the host cell.<sup>7</sup> Furthermore, the characteristic of 1-adamantanamine as a lysosomotropic weak base has been involved in the inhibition of the endocytosis of a virus.<sup>4</sup>

According to the endocytosis model, the attached virions are incorporated into endocytic vesicles in which a fusion of the virus and vesicle membranes occur when the pH of the vesicle is reduced. This fusion releases the virus into the cell cytoplasm, thereby, initiating the infection process. Researchers have proposed that the antiviral effect of lysosomotropic weak bases is due to their ability to interfere with this process. This has been illustrated by a study of the effects of lysosomotropic weak bases on the infection of baby hamster kidney cells by Sindbis virus.<sup>4</sup>

The lysosomotropic weak base, **1-adamantanamine**, probably acts by buffering the pH of endosomes, membrane-bound vacuoles that surround virus particles as they are taken into the cell. Prevention of



acidification in these vacuoles blocks the fusion of the virus and **endosome** membrane, therefore, the viral genetic material is not transferred into the cytoplasm of the cell and an infection does not occur.' Many studies have supported this concept concerning the importance of intralysosomal pH in the uncoating process of enveloped RNA viruses such as influenza A, rubella, parainfluenza 2 and 3, and lymphocytic choriomeningitis virus, and the inhibitory effect of amines on viral growth due to their neutralization of intralysosomal pH.<sup>13</sup>

The concepts just stated are the basis of this research project, which is the study of the **acid/base** characteristics of **1-adamantanamine** in aqueous, acetonitrile solutions using Fourier Transform Infrared Spectrometry. This  $pK_a$  study is performed with aqueous and mixed solvent solutions of varying hydrophobicity to investigate potential changes in  $pK_a$  upon membrane interaction of this antiviral agent.



## CHAPTER II

### HISTORY

#### Principles of Infrared Spectrometry

The infrared region of the electromagnetic spectrum includes radiation with wavenumbers within the range of 12,800 to  $10\text{ cm}^{-1}$ . This region of the spectrum is subdivided into near, middle, and far-infrared radiation. The limits of each region are 12,800 to  $4,000\text{ cm}^{-1}$ ,  $4,000$  to  $200\text{ cm}^{-1}$ , and  $200$  to  $10\text{ cm}^{-1}$  respectively. Many analytical applications are confined to the  $4,000$ - $670\text{ cm}^{-1}$  portion of the infrared region.<sup>14</sup>

Within the mid-infrared region, there are many absorption bands. These bands are attributed to the transfer of energy from the infrared radiation to the vibrational energies of particular bonds or functional groups in the molecules of the sample.<sup>15</sup> The frequency or wavelength of absorption depends on the relative masses of the atoms, the force constants of the bonds, and the geometry of the atoms.<sup>16</sup>

In order for a molecule to absorb infrared radiation, a molecule must undergo a net change in dipole moment as a consequence of its vibrational or **rotational** motion. In other words, the **vibration** of the molecule must produce an oscillating dipole moment so that there can be an electrical interaction between the molecule and the electric field of radiation.<sup>14</sup>

There are two basic types of molecular vibrations: stretching and bending. A stretching vibration is one in which there is a rhythmical movement along the bond axis such that the interatomic



distance is increasing or decreasing. The two types of stretching vibrations are symmetric and asymmetric. A bending vibration is one in which there is a change in bond angle between two bonds. The four types of bending vibration possible include scissoring, rocking, wagging, and twisting.<sup>16</sup> Figure 2 illustrates the various types of molecular vibrations.

All the vibration types are possible in a molecule containing more than two atoms. Also, coupling of vibrations may occur if the vibrations involve bonds to a single central atom. The result of coupling is a change in the characteristics of the vibrations involved.<sup>14,17</sup>

### Infrared Spectrum of a Substance

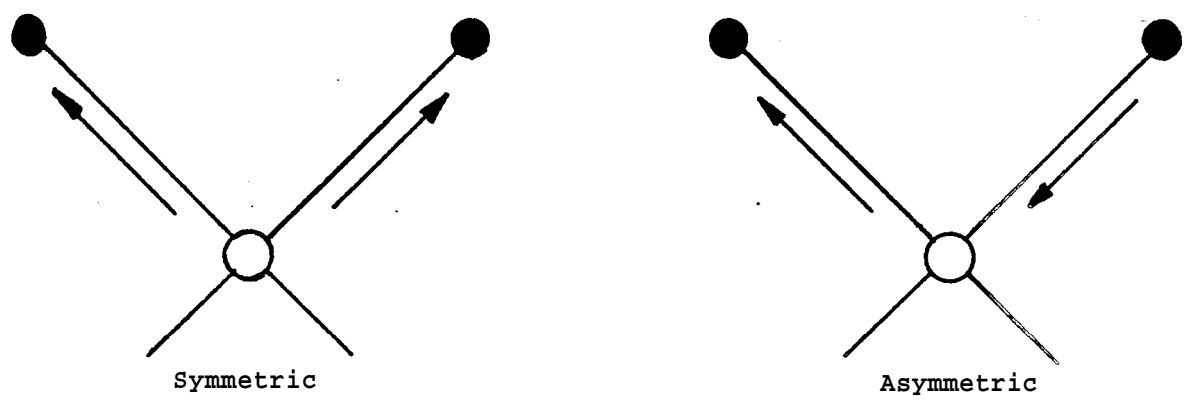
The infrared spectrum of a substance is the mapping of the molecule's vibrations. The spectral data consists of vibration frequencies and intensities of interaction with infrared radiation. Presence of various types of atoms, bonds, or functional groups is inferred by comparison with established group frequencies in correlation charts.<sup>18</sup>

Absorption band positions in infrared spectra are presented as wavenumbers or wavelengths. The wavenumber unit of  $\text{cm}^{-1}$  is most often used since it is proportional to the energy of the vibration.<sup>16</sup>

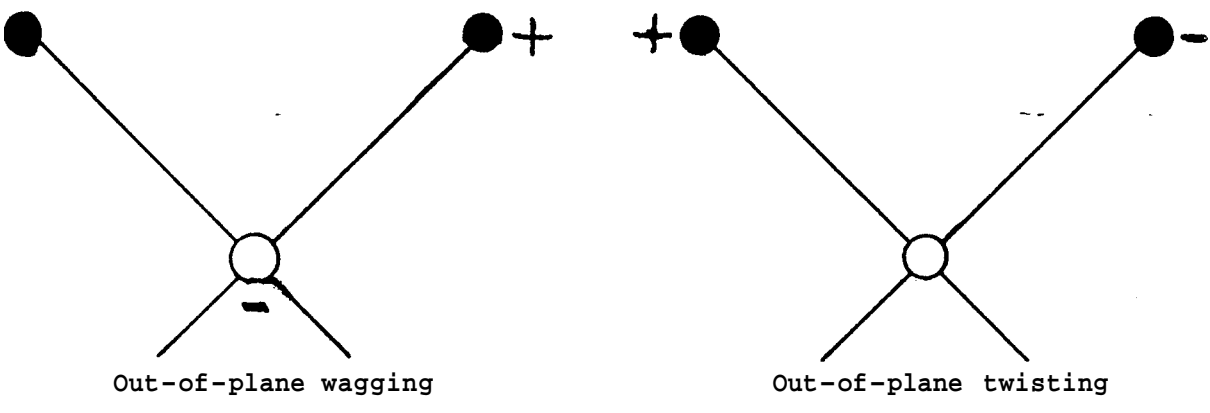
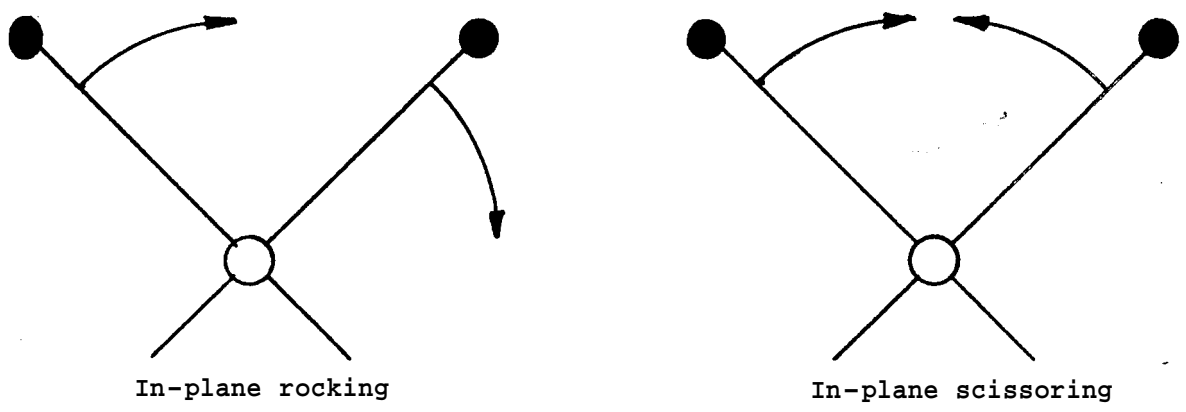
The band intensities are expressed as transmittance or absorbance. The ratio of the radiant power transmitted and the radiant power incident on the sample is transmittance. Absorbance is the logarithm of the reciprocal of transmittance.<sup>16</sup>







(a) Stretching vibrations



(b) Bending vibrations

Figure 2. Types of molecular vibrations. Note: + indicates motion from plane toward reader; - indicates motion from plane away from reader. 14



## Trends in Infrared Spectrometry

Infrared spectrometry has been used effectively in qualitative and quantitative analysis. Its most important use has been in the identification of organic compounds.<sup>14</sup> But in the 1970's, infrared spectrometry was felt to be a vanishing **technique**.<sup>19</sup> This soon changed due to the effect of computerization on all aspects of acquisition, processing and storage of data, and identification of spectra. These advances led to a resurgence in the use of infrared spectrometry especially Fourier Transform Infrared Spectrometry.<sup>16</sup>

## Theory of Fourier Transform Infrared Spectrometry

### INTRODUCTION

The technique of Fourier Transform Infrared Spectrometry allows all the frequencies of a broad region of the infrared spectra to be measured simultaneously. The frequencies which are seen at the detector create an interference pattern called an interferogram. This interferogram is then converted into spectroscopic terms utilizing fourier transformation, a mathematical operation.<sup>20</sup>

In practice, two interferograms must be recorded, **trãnsformed**, and ratioed to produce the transmittance or absorbance spectra which are useful in chemical analysis. The two interferograms necessary are the sample and the background interferograms. In addition, to improve the signal-to-noise ratio of the resultant spectrum, the interferograms from multiple scans are co-added before the fourier transform is performed to further reduce the noise.



All aspects of Fourier Transform Infrared Spectrometry will be discussed in detail in the upcoming sections. The theory behind this technique, the instrumentation involved, the advantages and disadvantages of the technique, and the history of the use of this technique with aqueous solutions will be reviewed.

### The Michelson Interferometer

Fourier transform infrared spectrometers utilize a scanning Michelson interferometer. The theory upon which this is based can be introduced by studying the two-beam interferometer first described by Michelson in 1891. The Michelson interferometer is a device which bisects a beam of radiation that later recombines after a path difference is introduced. The intensity variations of the recombined beams are measured by a detector as a function of path length differences.<sup>14</sup> This type of interferometer is demonstrated in Figure 3.

As shown in the figure, a beam of radiation is split by a beamsplitter into two equal halves. One half of the radiation is transmitted while the other half is reflected. The resulting beams are then reflected from a fixed mirror (at point F) and a moveable mirror (at point M).<sup>19</sup>

These beams then meet at the beamsplitter and interfere. Half of each beam is directed toward the detector and the other half of the beam is directed toward the source. Both of these output beams contain equivalent information; but the variation of the intensity of the beam passing to the detector as a function of the path difference is what produces the spectral information in a Fourier Transform Spectrometer.<sup>19</sup>



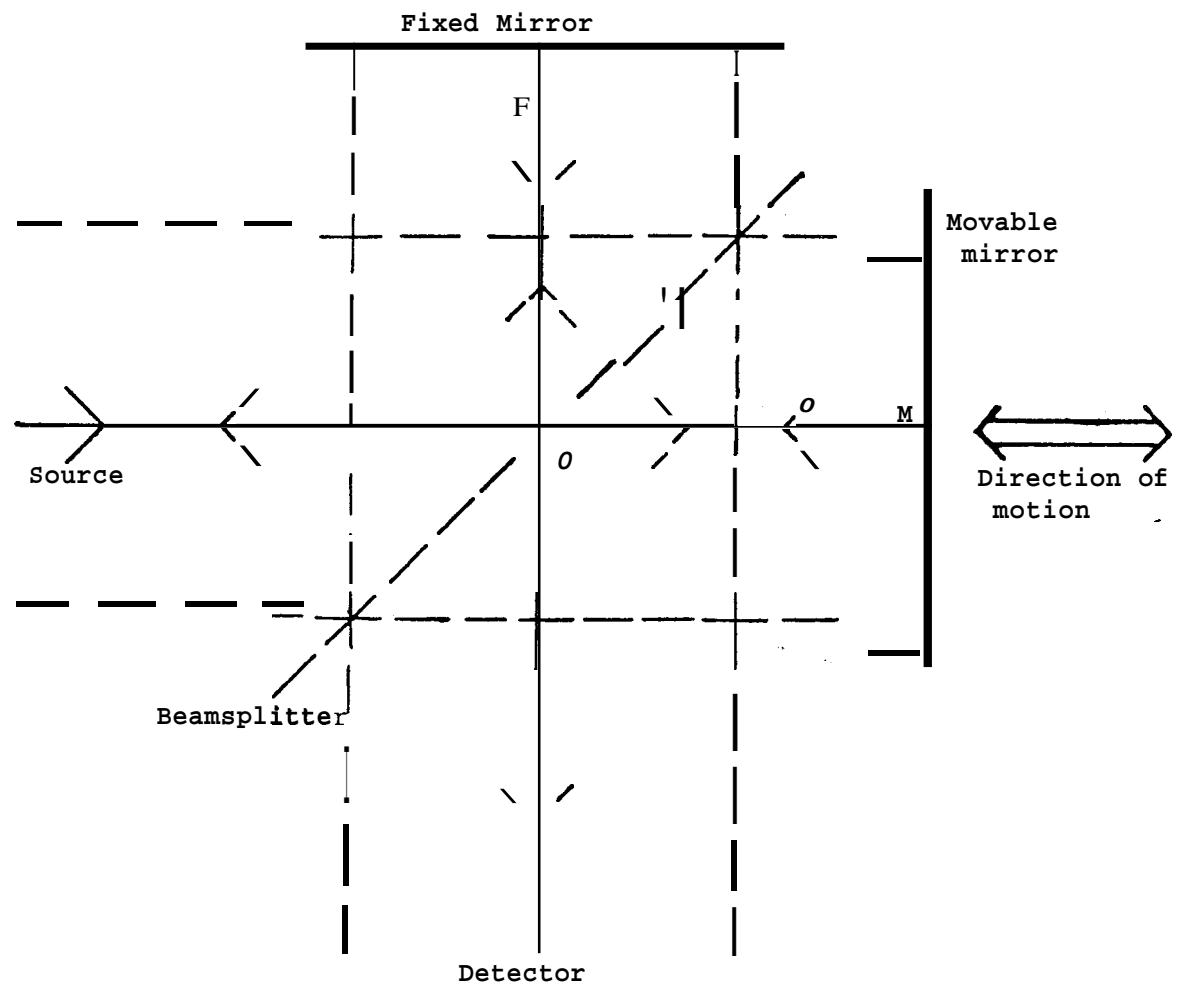


Figure 3. Schematic diagram of a Michelson interferometer. The median ray is shown by the solid line, and the extremes of the collimated beam are shown by the broken lines.<sup>19</sup>





The processes occurring in the Michelson interferometer can be illustrated by using an idealized situation in which there is a source of monochromatic radiation, producing an infinitely narrow, perfectly collimated beam. In this case, the beamsplitter is a nonabsorbing film with a transmittance and reflectance of fifty percent. The optical path difference between the beams traveling to fixed and movable mirrors is known as retardation. At zero retardation, when the fixed and movable mirrors are equidistant from the beamsplitter, the beams interfere constructively. In this situation, all the light reaches the detector and its intensity is the sum of the beams passing to the fixed and movable mirrors. On the other hand, when the retardation is  $1/2 \lambda$  cm the beams will interfere destructively and all the light returns to the source. Then at a retardation of  $\lambda$  cm the beams interfere constructively again. In addition, if the signal at the detector is measured as the mirror is moved at a constant velocity, it will vary sinusoidally with a maximum being measured each time the retardation is an integral multiple of  $\lambda$ .<sup>20</sup>

The interferogram can be calculated as a function of retardation and/or time. Several factors can affect the interferogram. These include the efficiency of the beamsplitter, the detector response, and the amplifier characteristics.<sup>19</sup>

From this interferogram the spectrum is derived by calculating the Fourier transformation. Fourier transformation is a mathematical procedure by which a digitized interferogram produces the spectrum.<sup>21</sup> The Fourier transform of a measured interferogram is a simple operation if the source is monochromatic light. If the source is emitting continuous radiation or several discrete spectral lines as for polychromatic sources, a digital computer is required to perform the calculation.<sup>20</sup>



## Types of Interferometers

There are two types of interferometers, slow scanning and fast scanning. The basic difference between these two types of interferometers is the scan speed of the moving mirror.<sup>20</sup>

Slow scan interferometers were used in the late 1960's for far-infrared spectrometry,  $6-600\text{ cm}^{-1}$ . Typical scan speeds are on the order of  $4\text{ }\mu\text{m}/\text{sec}$ . The usual technique for measuring spectrum with this technique involves modulating the beam with a mechanical chopper at frequencies between 10-20 Hz. This signal is amplified by a lock-in amplifier before it is digitized. An example of a slow scanning interferometer is a step scan interferometer in which the moving mirror is adjusted in a staircase fashion.<sup>20</sup>

The second type of interferometer available is the rapid scanning interferometer. It is used in the measurement of low or medium resolution mid-infrared absorption spectrum in which the interferogram has a high signal to noise ratio. The typical mirror velocity is  $0.158\text{ cm}/\text{sec}$ . Because of this high mirror velocity, the spectral frequencies are modulated in the audio-frequency range which then can easily be amplified using a band pass filter.<sup>20</sup>

## Sampling the Interferometer

Interferograms are measured, digitized, and stored in the computer until the fourier transform calculation can be made. The minimum number of resolution elements which can be sampled can be



calculated by the Nyquist Criterion. This rule states that any waveform that is a sinusoidal function of time or distance can be sampled at a frequency greater than or equal to twice the bandwidth of the system. At this frequency, the signal may be effectively recorded without any loss of information or detail.<sup>19</sup>

### Computing Techniques

As stated previously, once the interferogram is collected, the mathematical calculation known as the Fourier Transform must be performed in order to convert this information into a spectrum. There are now available several types of Fourier transform operations. Two will be discussed in this manuscript: the conventional method and the fast fourier transform method.

### Conventional Fourier Transform

Prior to 1966, a basic algorithm known as conventional, classical, or discrete fourier transform had been used to compute the spectrum from the interferogram. To perform this computation, each point is first multiplied by the corresponding point of an analyzing cosine wave and then the resultant values are added together. If the frequencies of the interferogram and the analyzing wave are the **same**, the resultant wave will be a large positive number. The magnitude of the sum will be proportional to the amplitude of the cosine wave interferogram.<sup>19</sup>



## Fast Fourier Transform

In 1965, **Cooley** and Tukey described an algorithm which has come to be known as fast fourier transform, FFT. In this method, the necessary computations are drastically reduced when compared to the classical fourier transform. The number of computations can be reduced because the discrete fourier transform of an interferogram of N points can be expressed in a general matrix form, and that matrix can be factored in a manner to reduce the overall number of computations.<sup>19</sup>

This reduction in the number of computations necessary to obtain a spectrum, can save the chemical spectroscopist a tremendous amount of time. In fact, most commercial systems have a microcomputer which can perform an 8192 point FFT in under 2 minutes.<sup>20</sup>

### Factors Affecting the Interferogram and Spectrum

Several parameters and mathematical operations can be performed on the interferogram and spectrum. These operations will change the appearance of the spectrum. -

#### Resolution

Resolution is a measure of an instrument's capability to distinguish between separate spectral lines of nearly equal wavelength.<sup>21</sup> In order to resolve the two lines, it is necessary to scan the spectrum long enough so that one complete beat frequency is complete. So an interferogram must be recorded from the point of zero retardation to the point where the two waves are again in phase.<sup>14</sup>





## Apodization

When a cosine wave interferogram is unweighted, the shape of the spectral line is due to the combination of the true spectrum and the sinc function. The sinc function is the transform of the boxcar truncation function. If a different weighting function is used, the instrument line shape will be changed.<sup>20</sup>

Apodization is the process of multiplying the interferogram by a weighting function, which suppresses the magnitude of the band side lobes. Apodization functions control the instrument line shape and act as a smoothing function, since the amplitude of the high spatial frequencies in the interferogram are reduced. When the absorption bands in the spectrum are broad, their spatial frequencies are low and less affected by an apodization function. In general, the overall effect of these functions is to improve the signal to noise ratio in the spectrum, but with a slight loss in resolution.<sup>21</sup>

The types of apodization available include boxcar truncation, trapezoidal, triangular, triangular squared, **Bessel**, cosine,  $\text{sinc}^2$ , Gaussian, and Happ-Genzel.<sup>19</sup> Of these, the most common apodization function used in Fourier Transform Spectrometry is the triangular apodization function. This method will reduce side lobes, but with a slight reduction in resolution and with some peak shape effects.<sup>21</sup> When this apodization is used, the background spectrum will not be affected since its interferogram has little information at large retardations. On the other hand, the narrow absorption lines will be apodized and have a new line shape.<sup>19</sup>



A second popular apodization function is the Happ Genzel function. The performance of this apodization function is similar to that given by triangular apodization.<sup>19</sup> An important feature of this function is that it most closely approximates the true spectral lineshape function showing correct linewidth and no storage side lobes.<sup>21</sup>

A third apodization function commonly used is the boxcar truncation. This function achieves the highest apparent resolution with no reduction in false sidelobes.<sup>21</sup> It has been noted that the use of this function will improve quantitative analysis.<sup>22</sup>

#### Smoothing

Smoothing the spectrum eliminates the effects of noise. There are many smoothing algorithms available, the most common method being boxcar integration. The basic premise for all smoothing functions is the calculation of a new value for the data using several data surrounding the original data points. The smooth function is performed by computing the fourier transform, multiplying by an apodization function, and computing the inverse transform. This function will make the data more pleasing to view; but, resolution is degraded by a factor of 2 or more.<sup>19</sup>

#### Baseline Adjustment

When spectra have baselines with continuous drift or slope, it may be necessary to perform baseline correction. This involves the elimination of the tilt and curvature of the spectrum. The tilt is a parameter to account for any constant offset in the baseline, and the curvature is the slope of the baseline.



## Spectral Subtraction and Addition

Spectral subtraction or addition is used to obtain a more accurate display of a spectrum of components in a mixture or to observe changes following a treatment of the **sample**. This is accomplished by determining sample and reference spectra, then multiplying the reference spectrum by a scaling factor, and then performing the addition or subtraction.<sup>21</sup>

## Fourier Transform Infrared Spectrometers Instrumental Design

All Fourier Transform Infrared Spectrometers consist of four basic systems. These include the interferometer and detector system, the data acquisition and optics control system, a general purpose computer, and the operator interface. A block diagram of these components is illustrated in Figure 4.<sup>23</sup>

## Interferometer Design and Drive Systems

The simplest version of the Michelson interferometer is composed of two plane mirrors with a beamsplitter between them where ~~one~~ mirror can move in a direction perpendicular to the plane of the other mirror.<sup>19</sup> The bearing support for the moving mirror must be discussed in detail because the bearing has a direct effect on the operating resolution, bandwidth, and applications of the FTIR analyzers. There are four types of bearings available: air bearing, oil bearing, flex point, and ball slide.<sup>23</sup>



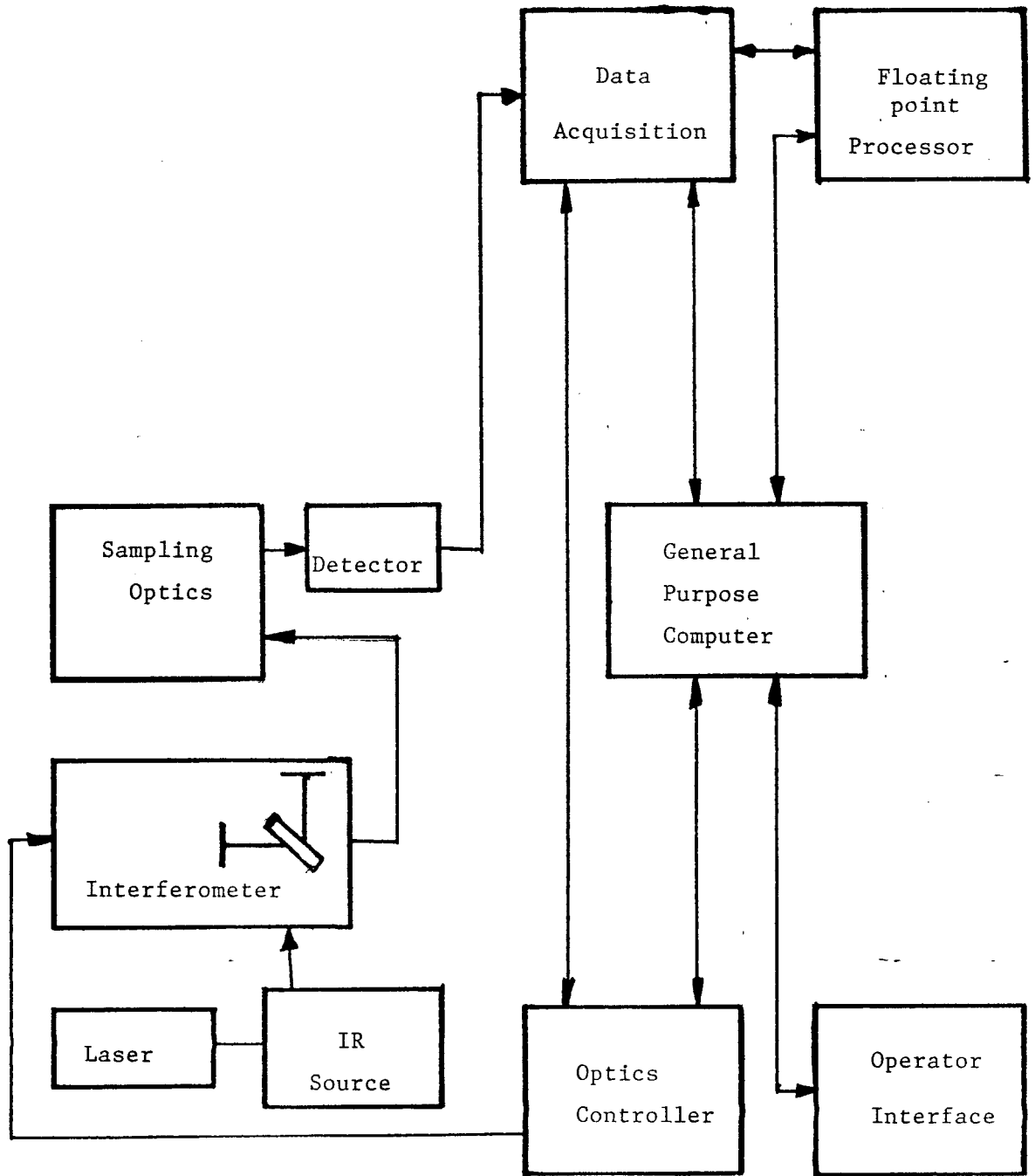


Figure 4. Block diagram of FTIR analyzer. 23





Most research-grade instruments employ an air bearing support which provides excellent mechanical performance, high resolution, and has the widest field application. One drawback is that it requires a high quality source of air or nitrogen.<sup>23</sup>

The second type of bearing, the oil bearing, is rarely incorporated into Fourier Transform Infrared Spectrometers. This bearing will provide about the same flexibility and advantages as the air bearing.<sup>23</sup>

Flex pivot bearings are used in low resolution instruments. They are inexpensive, but the maximum resolution attainable with this bearing is four wavenumbers.

The ball slide bearing is used when the interferometer is constructed with corner cube reflectors. This bearing provides high resolution at a low cost. The major disadvantage of this bearing is that its operation may produce acoustic interference.<sup>23</sup>

Another important component of the interferometer is the **moving-mirror** drive mechanism. The higher the resolution and maximum wavenumber in the spectrum, the higher must be the quality of the drive mechanism. The crudest drive mechanisms available are used in interferometers for far-infrared spectrometry at low or medium resolution of the slow scanning or stopped-scan variety. Medium resolution mid-infrared interferometers are rapid scanning and operate by signal averaging repetitive scans. The earliest mirror drive mechanism was a spring mount which was displaced by an electromagnetic transducer. Later, higher resolution systems were designed in which the



main interferometer was attached to the moving mirror of a reference interferometer which was triggered by monochromatic light. More recent advances utilize a microcomputer-controlled drive in which the position of the moving mirror is monitored throughout the measurement by continuously keeping a record of the fringes of a laser reference interferogram.<sup>19</sup>

#### Sources for Fourier Transform Spectrometers

The common sources employed in mid-infrared spectrometers include the Globars, Nernst glowers, and nichrome coils. Most **research-**grade instruments incorporate the Globar (silicon carbide) source which is usually water cooled.<sup>19</sup>

#### Infrared Detectors

Infrared detectors employed in Fourier Transform Infrared Spectrometers are either thermal detectors or quantum detectors. Thermal detectors operate by sensing the change of temperature of an absorbing material with the output obtained from a thermocouple, bolometer, thermistor bolometer, pneumatic detector, or **Golay** detector. The most commonly used thermal detector is the room temperature pyroelectric bolometer, DTGS detector, composed of deuterated triglycine sulfate.<sup>19</sup>

Quantum detectors detect infrared radiation based on the interaction of radiation with the electrons in a solid which cause electrons to be excited to a higher energy state. The most commonly used detector in this category is the mercury cadmium telluride



detector, MCT. This detector makes use of the properties of a mixture of two semiconductors to excite electrons from one state to another. It must also be maintained at liquid nitrogen temperatures.<sup>19</sup> The MCT detector has a higher degree of sensitivity and superior performance at higher modulation frequencies.<sup>23</sup>

#### Data Systems

Before the 1970's, the time savings gained due to the simultaneous measurements of all wavelengths was not realized to its fullest extent because of the time delays involved in the computation of the spectrum from the interferogram. Interferograms had to be recorded on magnetic tape and transferred to the computer center for calculation of the spectra. And, when spectral data was required immediately after data collection, the interferogram had to be analyzed using an audio-frequency wave analyzer and an XY plotter.<sup>19</sup>

Then in the 1970's, stand-alone fourier transform infrared spectrometric systems became available with microcomputers. Most microcomputers operate under a file management system in which all data and programs reside in a mass storage unit, usually a magnetic disk. The computer functions under an operating system that performs most operations. This system is flexible and allows multitasking.<sup>-19</sup>

As the capabilities of the microcomputers have increased, the speed with which computations are completed, the speed at which memory is accessed, and the memory space have all increased. Also included as basic hardware is a keyboard to communicate with the instrument, a video display, a hard disk drive, and a hard-copy plotter.<sup>19</sup>



In addition, some instruments will have an interface system which employs automated function keys. These keys can be used to automate some of the procedures. An example of such a key exists in the system used in this work for baseline correction. By using the automated function keys for this procedure, the computer chooses the ideal points to be used for the baseline determination, calculates the corrections, and displays the corrected spectrum.<sup>24</sup>

#### Sampling Techniques-Cylindrical Internal Reflection

One technique available for sample analysis is internal reflectance spectroscopy. This technique involves passing the infrared radiation through an infrared transmitting crystal of high refractive index, and allowing the radiation to reflect off the crystal after extending slightly into the solution.<sup>25</sup> The use of a cylindrical internal reflection element is the basis of the cylindrical internal reflection. The advantage of this technique is optical matching of the interferometer beam and crystal geometry and easy processing of liquids. Wilks has proposed a useful design utilizing a crystal rod with polished cone-shaped ends. Figure 5 illustrates this design. It is known as the circle accessory and permits the incoming infrared rays to be directed to the cylindrical surface at the desired angle of incidence.<sup>25</sup> - -

Useful crystal materials include zinc selenide, germanium silicon, sapphire, and zinc sulfide. This crystal rod is sealed within the sample chamber. This chamber had been designed to provide a free flow of sample so that it fills without trapping bubbles and empties completely. When a sample is measured, the solutions must cover the entire crystal rod completely.<sup>25</sup>





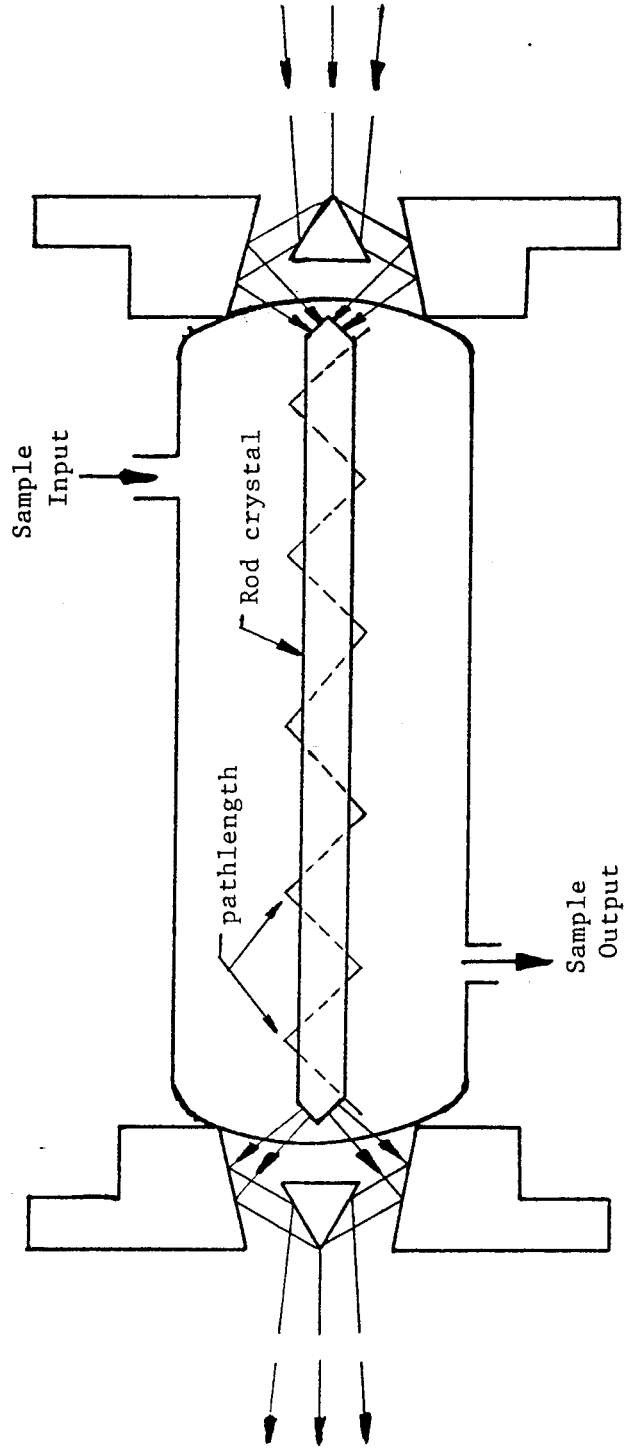


Figure 5. Optical diagram of the Flow-thru Circle Cell. 25



This circle accessory is useful for the fourier transform infrared analysis of strongly absorbing liquids, solutions, and mixtures. When water is used as a solvent it is difficult to perform FTIR determinations because of water's highly absorbing nature. Because of this fact, the presence of highly absorbing bands such as the OH stretch in the region of  $3200\text{ cm}^{-1}$  tend to obscure the weaker more interesting bands. This problem is overcome using the circle accessory due to the pathlength through the **solution**.<sup>26</sup> The pathlength utilized by this type of accessory is in the range of 3.6-21  $\mu\text{m}$  depending on the wavelength.<sup>25</sup> At this pathlength, concentration of 0.5% of moderately absorptive samples are detectable and yield reliable information in the  $3200\text{-}750\text{ cm}^{-1}$  range.

#### Advantages of Fourier Transform Infrared Spectrometry

Fourier Transform Infrared Spectrometry has several inherent advantages which make it a useful analytical technique. These advantages include Fellgett's advantage, Jacquinot's advantage; continuous calibration, and the utilization of microcomputers.

Data from all spectral frequencies can be measured simultaneously with the same detector. This advantage known as the multiplex advantage or Fellgett's advantage permits the measurement of many components in a single stream without mutual interference, identification of impurities not targeted for analysis, and the ability to analyze compounds in the presence of water.<sup>14,23,27,28</sup>



Another advantage of this instrumental technique is the absence of slits and filters. This is known as Jacquinot's advantage.<sup>21</sup> Because of this, the maximum allowed throughput is not influenced by the slit height and grating constant. The source energy is not limited by the use of slits. Therefore, the intensity of the infrared radiation reaching the detector is greater than with dispersive instruments. Due to this increased throughput, mixtures which are too opaque or complex for conventional dispersive techniques can be measured.<sup>27</sup> In addition, high resolution is obtainable because the resolution can be easily controlled by the use of apodization techniques.<sup>28</sup>

Continual internal calibration of the scanning mirror is another advantage of this instrumental technique. This calibration is performed by an internal laser. Due to this calibration, the data collected is more accurate and precise than other techniques because the laser signal determines sampling intervals and the point at which data collection should begin between successive scans.<sup>28</sup>

In addition, the utilization of microcomputers and automation make this technique more useful, easier to manipulate, and more cost effective. Microcomputers have permitted more rapid spectra generation from **interferograms** due to the rapid performance of mathematical computations. Also, data manipulation such as baseline correction, smoothing, and subtraction can be performed now due to increased computer power and storage capability. All of these factors plus the saving of the chemist's time decrease the cost of the use of this instrumentation.



### Disadvantages

There are several points in which there is a trade-off in accuracy and convenience. These disadvantages include a decrease in accuracy due to approximations employed in computer calculations, the sensitivity of the instrument to temperature and vibrational changes, and alignment of the instrument's components.

Computers are used to simplify the processing of fourier transform data. The rapid performance of these calculations may lead to a decrease in accuracy. Small peaks may be lost due to round-off and scaling errors. Peak appearance may be altered due to certain calculations such as baseline correction and subtraction. Also, problems may arise in peak detection if the computer program utilizes an interpolation process.<sup>29</sup>

In addition, Fourier Transform Infrared Spectrometers are sensitive to heat extremes. Temperature affects the optical performance by degrading the interferometer **alignment**, the infrared source, and the infrared detectors. Therefore, a temperature-controlled housing is necessary. This decreases the convenience of the technique and significantly increases the cost of the instrument.<sup>23</sup>

The Fourier Transform Infrared Spectrometer is also **sensitive** to vibrations in the 50-300 Hz range. This is due to the fact that the infrared signal is modulated at similar frequencies. Thus, such vibrations must be eliminated or the quality of the infrared spectrum will be affected.<sup>23</sup>





Also, the quality of the spectrum may be affected by misalignment of the fixed mirror relative to the moving mirror. In addition, the accuracy of the maintenance of the plane of the moving mirror during scanning will affect spectrum appearance. Another factor which influences the shape of the spectrum, is the quality of the drive mechanism used for positioning the moving mirror.<sup>19</sup>

A disadvantage which must also be mentioned when cylindrical internal reflection techniques are used is that this is a low light throughput technique. This means the percent of energy passing through the accessory without sample is only 10-20% of the open beam throughput. For this reason, the intensity of infrared radiation reaching the detector is decreased, and, high resolution may not be obtained.

Another problem which accompanies cylindrical internal reflection accessories is the cell's pathlength. This pathlength is an advantage but also limits the detection of substances in minute concentration. Usually, a concentration of 0.5% of moderately absorptive sample is the lower limit of detection. It must be mentioned that this lower level of detection can be decreased to 0.05 to 0.1% by using a MCT detector.

#### Summary of the Fourier Transform Infrared Spectrometry of Aqueous Solutions

Infrared spectrometry has not been widely used in the fields of biochemistry or medicine because most measurements in this area require an aqueous solvent. Traditionally, it was difficult to measure **aqueous** solutions because the intense water absorption bands obscure most of the



mid-infrared spectrum. Although water does absorb infrared radiation strongly, fourier transform infrared spectra of samples dissolved in water are not particularly difficult to measure provided a cell with the proper pathlength is used. It has been noted that cylindrical internal reflectance elements provide a short enough pathlength for the infrared spectroscopy of aqueous solution from 3200 to 800  $\text{cm}^{-1}$ .<sup>30</sup>

This technique is now used to perform qualitative and quantitative studies on aqueous solutions. Qualitative studies which have been performed include an evaluation of aqueous antibiotic solutions by Rein and Wong. The characteristics of five percent oxacillin were shown to have absorption bands associated with the beta-lactam carbonyl group plus bands due to other components in the mixture. Another study by **Mathias**, involved the determination of the spectra of water-soluble polymers such as polyacetamidoacrylic acid.<sup>25</sup>

Both of these groups later performed quantitative studies. Wong and Rein measured the spectra of solutions of varying concentration of the beta **lactams** in aqueous solutions.<sup>30</sup> **Mathias** studied various concentrations of glycine in water solutions. Both groups discovered that there was an excellent Beer's law relationship.<sup>25,30</sup> Other studies include the analysis of shampoo formulations by Sabo, Gross, and Rosenberg, of fermentation broths containing methanol, ethanol, and acetone by Kuehl and Crocombe, and cow's milk by Goulden.<sup>25</sup>



Because of the success these researchers had in the measurement of aqueous solutions, the advantages of using cylindrical internal reflectance, and the advantages of Fourier Transform Infrared Spectrometry previously listed, it was decided to determine the qualitative differences of aqueous acetonitrile solutions of **1-adamantanamine** at various pH concentrations. The spectral similarities and differences will be analyzed and the  $pK_a$  values of the drug as a function of acetonitrile content will be determined.



## CHAPTER III

### APPARATUS AND MATERIALS

#### IR/32 FTIR Spectrometer

The IR/32 is a single-beam rapid scanning mid-infrared range spectrometer manufactured by IBM Instruments, Inc. The standard system consists of an operator's console and an optics bench. Figure 6 is a block diagram of the main assembly.<sup>21</sup>

The operator's console controls the optics bench and performs all the mathematical functions. It includes a twelve-inch display, a pushbutton keypad, an eight-inch diskette drive, a hard disk drive, and a XY 749 printer/plotter. The data system is run by an IBM system 9000 microcomputer with IR/32 executive software.

The optics bench houses the infrared source, helium-neon laser, interferometer, sample compartment, and infrared detector. This bench requires a dry, oil free air or nitrogen supply for the purge and air bearing. Also a self-contained heat exchanger and circulating pump unit provides a water cooling system to carry away excess heat from the source and power supply. A schematic diagram of the optics bench is illustrated in Figure 7.<sup>21</sup>

Infrared light from the helicoil globar source (A) is directed into the Michelson interferometer consisting of a beamsplitter (C), fixed mirror (D), and moving mirror (E). The moving mirror is mounted on a rectangular air bearing which moves at a constant velocity because of a linear induction motor. The infrared radiation from the interferometer passes through the sample compartment with a focus at





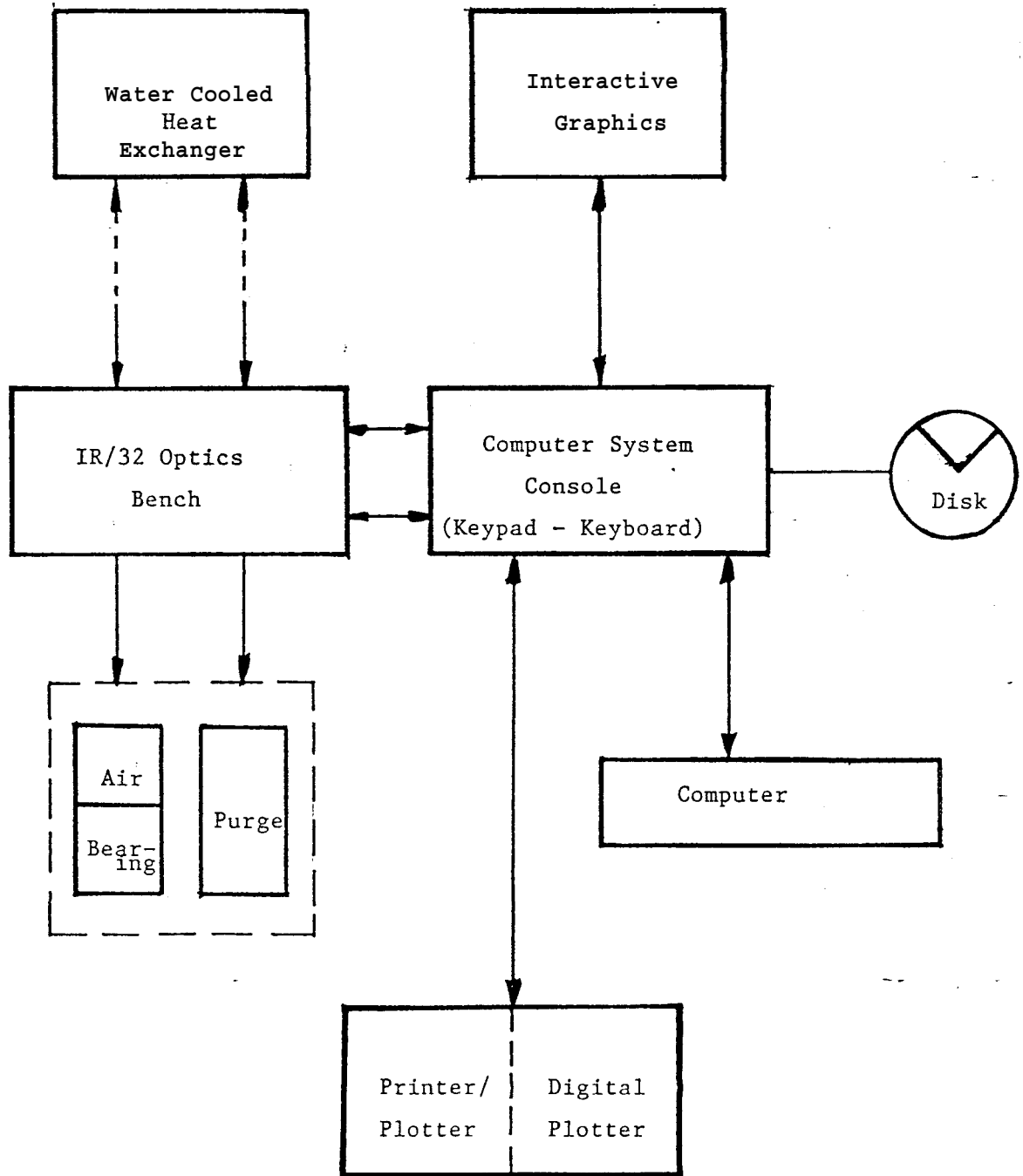


Figure 6. Block diagram of the IR/32 main assembly.<sup>21</sup>



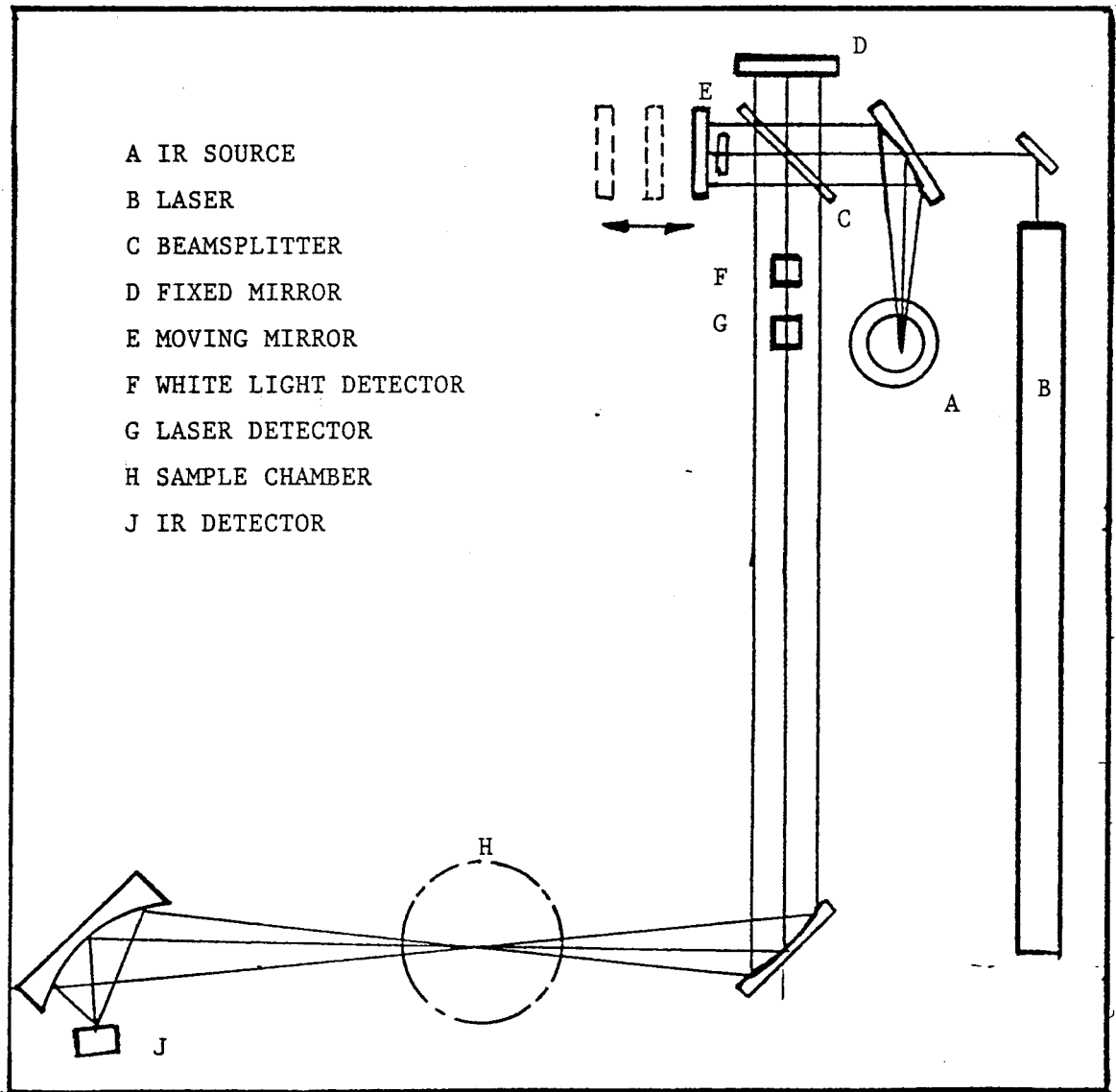


Figure 7. Schematic diagram of the IR/32 Optics Bench.<sup>21</sup>



position H. The radiation is then focused onto the infrared detector (J). In this case a liquid nitrogen cooled mercury-cadmium telluride detector was used. Also light from a helium-neon laser (B) follows the same path and is detected by the laser detector.<sup>21</sup>

A cylindrical internal reflection accessory was used for the measurement of the aqueous, acetonitrile solutions. The circle accessory was a 3-mL flow-thru cell containing a 1/4" diameter zinc selenide internal reflection crystal. A diagram of the circle accessory is in Figure 8.<sup>26</sup>

#### pH Meter

The Orion Model SA 520 pH Meter (Orion Research Incorporated, 529 Main Street, Boston, Massachusetts 02129, Catalog Number SA-520) was used to measure the pH of the aqueous, acetonitrile solutions. This instrument is a microprocessor controlled pH meter with a touch-sensitive keyboard for fast, convenient, and reliable pH, electrode potential, and concentration measurements with automatic temperature compensation.<sup>31</sup>

#### Combination pH Electrode

An Orion micro **glass/reference** combination electrode<sup>-</sup> was used (Orion Research Incorporated, 529 Main Street, Boston, Massachusetts, 02129). The glass and calomel reference electrode are combined in one tube with a saturated potassium chloride filling solution.<sup>32</sup>



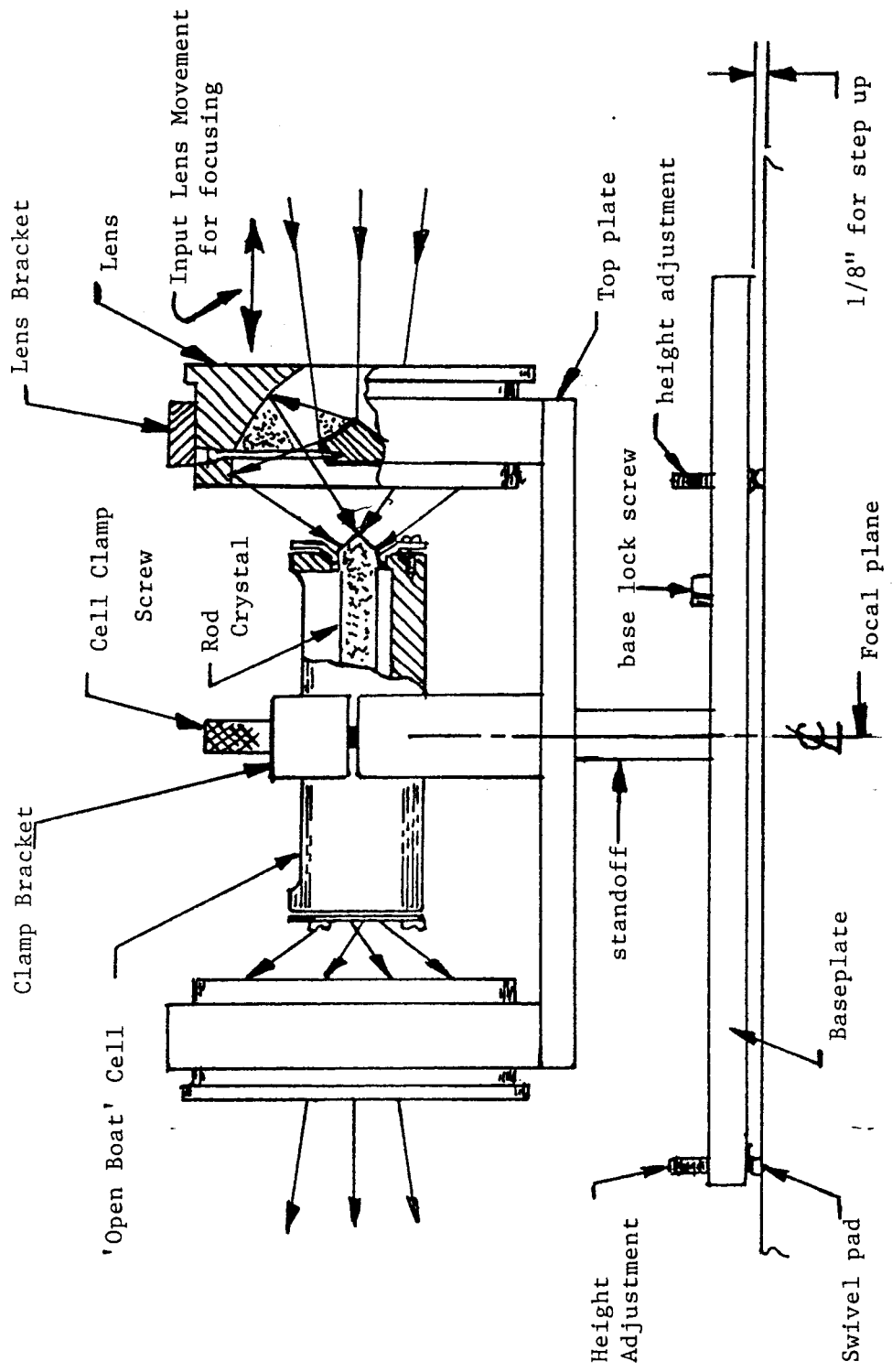


Figure 8. Diagram of a Circle Cell Accessory. 26





Chemicals

The following chemicals or solutions were purchased for use in this research project.

- A. Fisher Scientific (Fisher Scientific, 711 Forbes Avenue, Pittsburgh, Pennsylvania, 15219) provided:<sup>33</sup>
1. Buffers pH 7, 4, and 10 (catalog numbers 50-b-101, 107, and -111).
  2. Hydrochloric Acid, A.C.S. reagent (catalog number A144-500)
  3. Sodium hydroxide, anhydrous pellets (catalog number 318-100)
- B. Aldrich Chemical Company (Aldrich Chemical Co., P.O. Box 355, Milwaukee, Wisconsin, 53201) provided:<sup>34</sup>
1. Acetonitrile, **99+%**, spectrophotometer grade (catalog number 15-460-1).
  2. **1-Adamantanamine**, 95% (catalog number 13857-6).



## CHAPTER IV

### EXPERIMENTAL METHODS

#### Introduction

This experiment involves the determination of the infrared spectra of various aqueous, acetonitrile solutions of **1-adamantanamine** to denote the changes which occur in the structure of this compound as a function of pH and solvent composition, Once these spectra are determined, they are manipulated by using the baseline adjustment, smoothing, and peak picking functions available with the **FTIR/32**. Then the absorption bands common in all solutions are used to determine the  $pK_a$  of the drug in aqueous and mixed solvents.

#### Part A: Preparation of Reagents

Initial set-up of this experiment involved the preparation of the following solutions:

1. 0.6 N solution of Hydrochloric Acid
2. 5 M solution of Sodium Hydroxide
3. 25% Acetonitrile Solution in Water
4. 50% Acetonitrile Solution in Water
5. 75% Acetonitrile Solution in Water
6. 0.013 M Solutions of **1-adamantanamine** in water, 25% acetonitrile, 50% acetonitrile and 75% acetonitrile



## Part B: Flow-thru Cell and Pump Set-up

A flow-thru cell connected to a circulating pump is utilized. The cell is inserted into the FTIR. The input hose to this cell originates from the reaction beaker containing the test solution. The output hose from this cell leads to the same reaction beaker. This beaker also contains the combination pH electrode. Figure 9 illustrates this set-up. Because of this set-up, the various solutions can be pumped through the flow-cell continuously as the pH is adjusted. Once the pH stabilizes at the desired interval, the pump is turned off and the spectrum of the solution is determined.

## Part C: FTIR Measurement of Samples

### Standard Operating Procedure

A standard operating procedure should be established using the options function to set the parameters one wishes to employ. This procedure should include the following information: resolution, number of scans, type of apodization, detector type, plot device, wavenumber boundaries, and transmittance and absorbance boundaries. The parameters used in this experiment are listed in Table 1. Once these parameters are set, this procedure should be given a name and saved. Thereafter, each time the instrument is turned on, this operating procedure can be recalled.



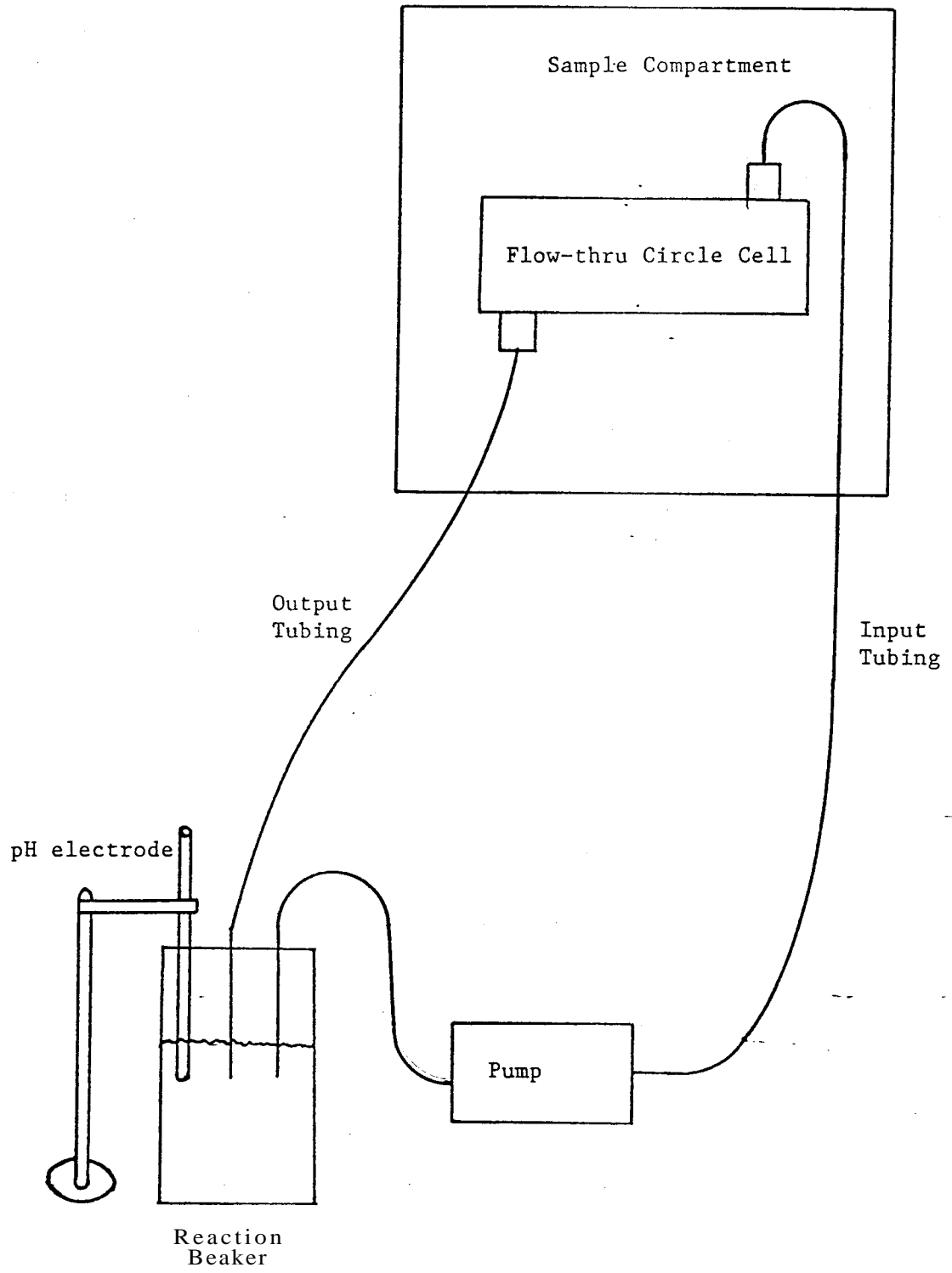


Figure 9. Flow-thru cell and pump set up.





TABLE 1

## INSTRUMENTAL SPECIFICATIONS USED DURING THIS PROJECT

Resolution	2 cm <sup>-1</sup>
Scan counts	64
System Parameters	
<b>Apodization</b> method	Triangular
Correlation for Data Collection	Low
Detector Type	MCT
Keyboard Enabling	Enabled
Plot device	IBM Instrumewnts XY/749
Data Processing Parameters	
Smooth	<b>Savitzky-Golay</b> Smooth activated
Number of passes	1
Number of points spanned	7
Peak Pick Generation of Peak Table	
Peak table limits(number of points)	20
Peak sort qualifier	Decreasing wavenumber
Display Control Parameters	
High frequency limit	3100.00
Low frequency limit	1000.00
% Transmittance Maximum	100.00
% Transmittance Minimum	0.0
Absorbance Maximum	.8
Absorbance Minimum	-.02
File	
Default Disk Drive Presently	Drive #4 (hard disk) Soft disk #0
Automatic File Name Generation	Disabled
Default Operator Name	Baca
Default Sample Name	<b>1-adamantanamine</b>
Default Sample Descriptor	Flow-thru Circle cell
Set Quarry for file save	Enabled



## Collection of Background and Sample

Before a sample spectrum can be collected, a background spectrum of the solvent used as the diluent for the drug must be collected. These two interferograms must be recorded, transformed and ratioed to produce the absorbance spectrum. The absorbance spectrum is desired in this project because most procedures used in the manipulation of data require this mode. The following sequence can be utilized when collecting background and sample spectra:

1. Load the Standard Operating Procedure using the **Load/Save** function of the options keypad command sequence.
2. Install the flow thru cell. Pump through this cell the background solution consisting of the solvent system and **1-adamantanamine**. Background spectra to be collected include **1-adamantanamine** solutions in water, 25% acetonitrile, 50% acetonitrile, and 75% acetonitrile solvents at acidic condition, pH 2.
3. Collect the background spectra by using the keypad command, collect-background.
4. Once an acceptable background, small  $\text{CO}_2$  and water absorption peaks, is established, the pH should be adjusted to the next interval by the addition of **NaOH**. The circle pump will pump this solution through the flow cell for fifteen minutes. At the end of this waiting period, the pump should be turned off. Intervals which are tested include pH 5, 6, 7, 8, 9, 10, 10.5, 11, 11.5, 12, 12.5 and 13.
5. The sample spectrum of each aliquot can be determined by using the keypad command "sample."



6. Nine sample spectra are collected and co-added together using the addition mode of the FTIR/32 to obtain a spectrum with increased resolution and decreased noise level.

#### Part D: Manipulation of Spectral Data

Once the sample and background spectra have been collected, it is necessary to manipulate the absorbance spectra using the baseline adjustment and smoothing functions. In addition, the absorption peaks which were common to all solutions are identified using the cursor keypad command sequence. The minimum and maximum absorbance of each peak at the various pH concentration are determined. These net changes in absorbance will then be used to calculate the  $pK_a$  of the drug in the various solutions.



## CHAPTER V

### EXPERIMENTAL RESULTS AND DISCUSSION

#### Introduction

Fourier Transform Infrared Spectrometry was used to study the **acid/base** properties of **1-adamantanamine** in varying solvents and pH. The effect of solvent and pH on this compound in water and 25, 50, and 75% acetonitrile solutions was studied by noting the net absorbance of the infrared absorption bands common to all spectra as the pH was adjusted from acidic conditions to alkaline conditions. This was done after a background spectrum at pH 2 was obtained. By using pH 2 solutions as the background, any absorption band changes within the ranges of 3100-1000  $\text{cm}^{-1}$  which occurred as the pH of the solutions became more alkaline could be monitored. The aqueous and acetonitrile solvents did not influence these spectra because the background absorbances are subtracted out of the sample spectra.

Two major absorption bands, peak A and peak B, appeared consistently in all the **1-adamantanamine** solutions as the pH became more alkaline. The **ranges** for these peaks were established. In all solutions tested, peak A occurred in the 2939-2900  $\text{cm}^{-1}$  range, and peak B occurred in the 2866-2843  $\text{cm}^{-1}$  range. Figures 10, 11, 12, and 13 illustrate the characteristic infrared spectra of **1-adamantanamine** in water and 25, 50, and 75% acetonitrile solutions under alkaline conditions, pH 11.





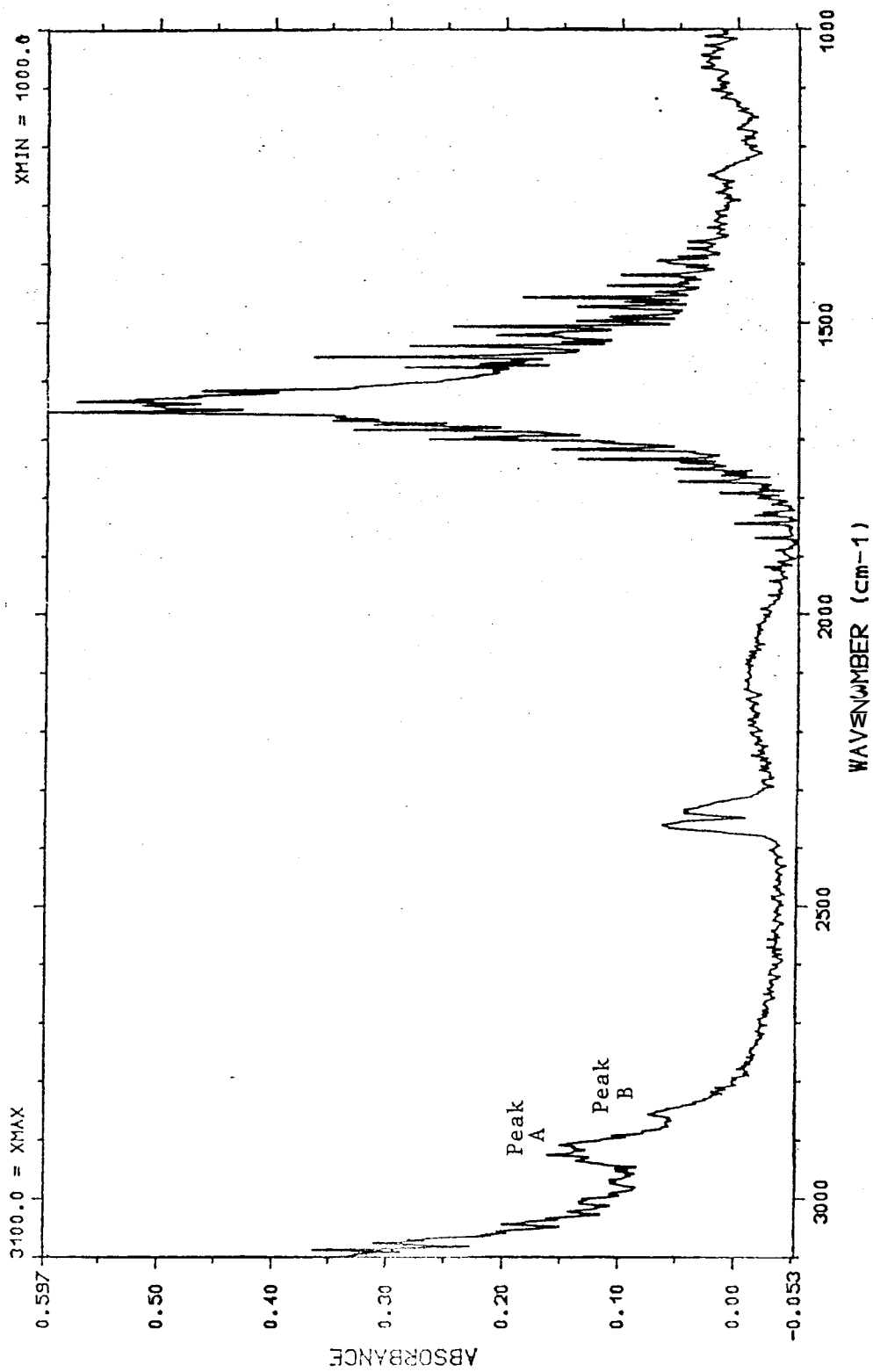


Figure 10. SAMPLE NAME : 1AD AMANTAMINE IN WATER AT PH 11  
SAMPLE FORM : FDW -THRU CIRCL 2 CELL  
OPERATOR : BSE /ANN BACA



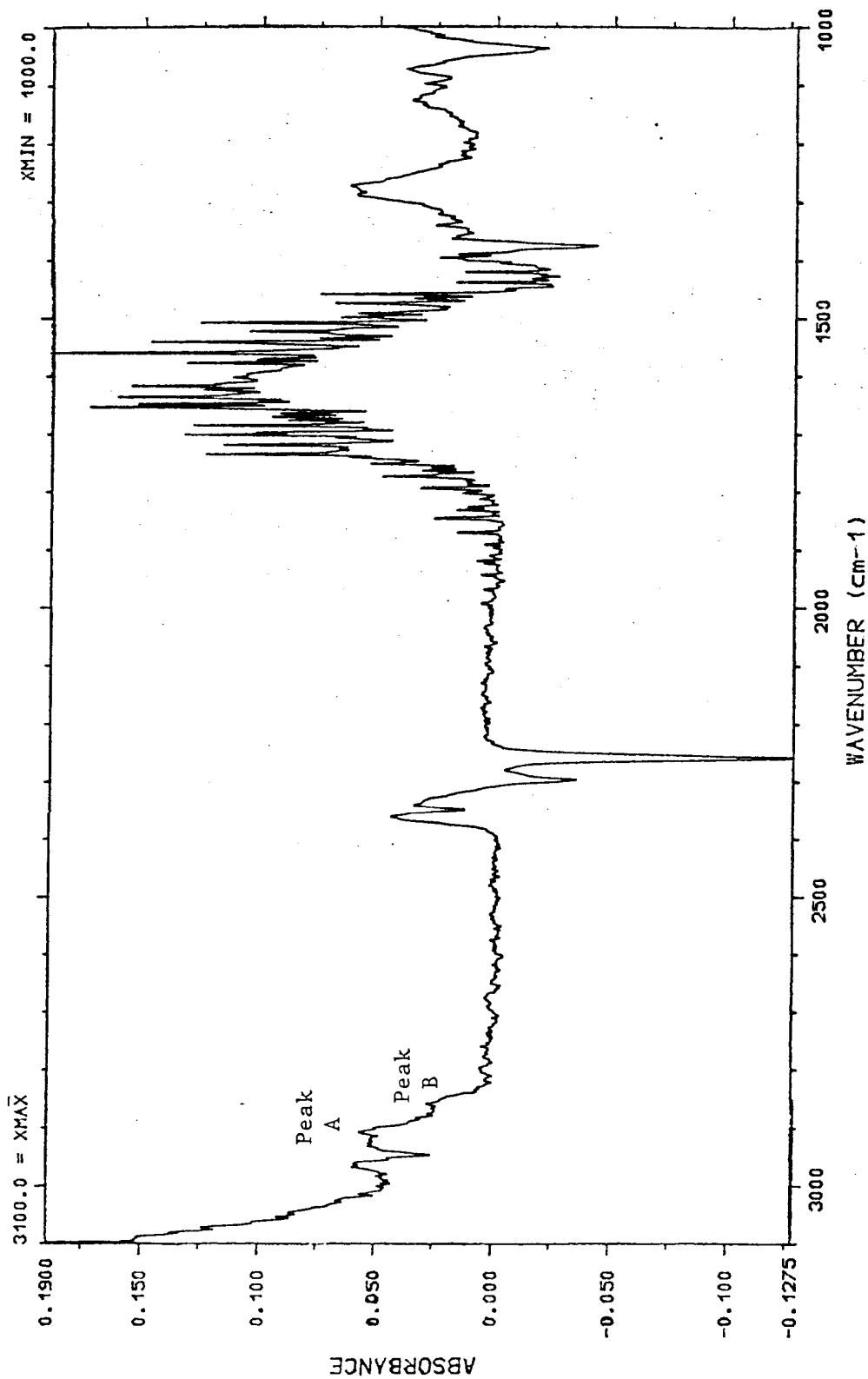


Figure 11. SAMPLE NAME : 1-ADAMANTANAMINE IN 25% ACETONITRILE AT PH11  
SAMPLE FORM : FLOW-THRU CIRCLE CELL  
OPERATOR : ROSEANN BACA



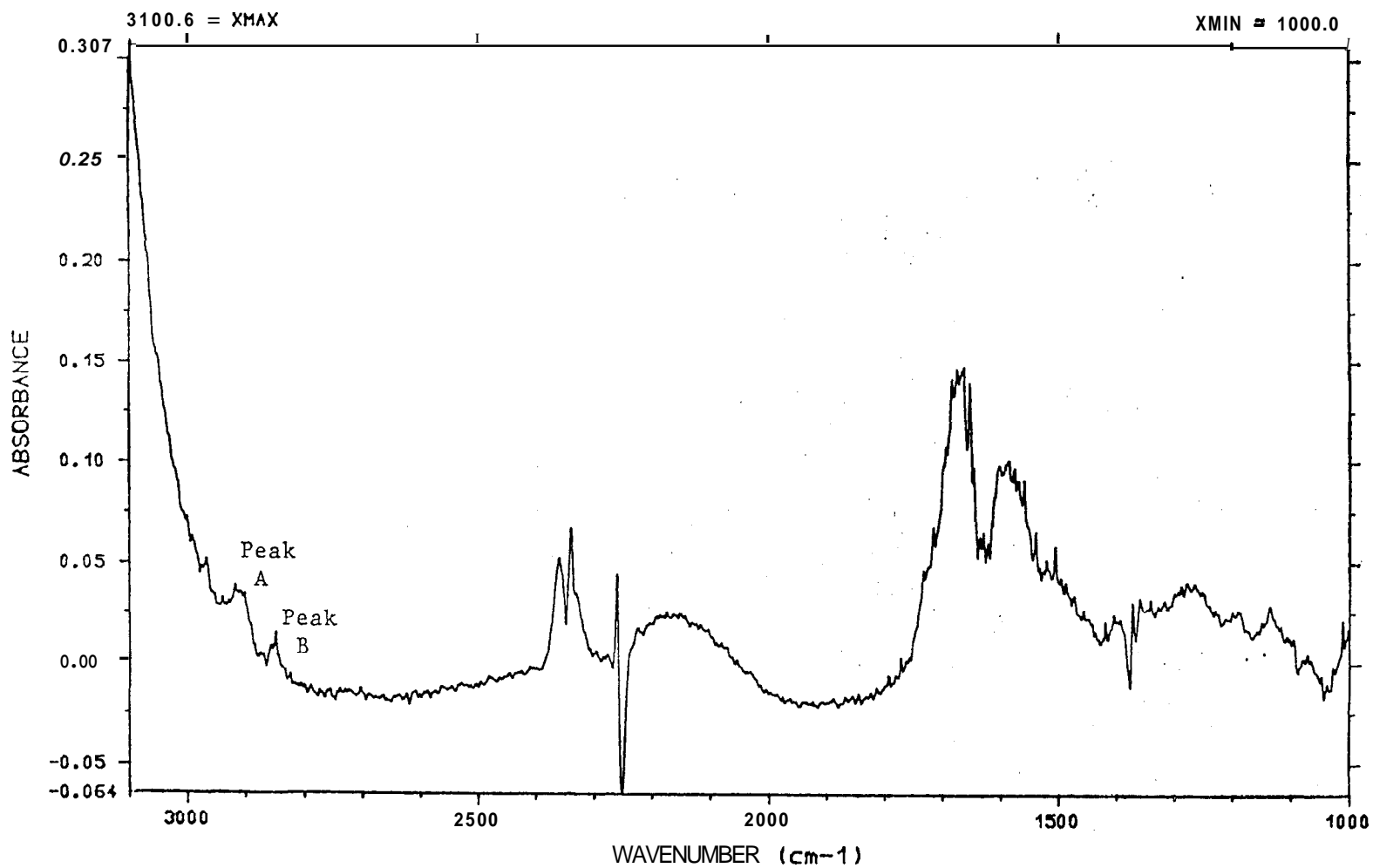


Figure 12.

SAMPLE NAME : 1-ADAMANTANAMINE IN 50% ACETONITRILE AT PH 11  
SAMPLE FORM : FLOW-THRU CIRCLE CELL  
OPERATOR : ROSEANN BACA



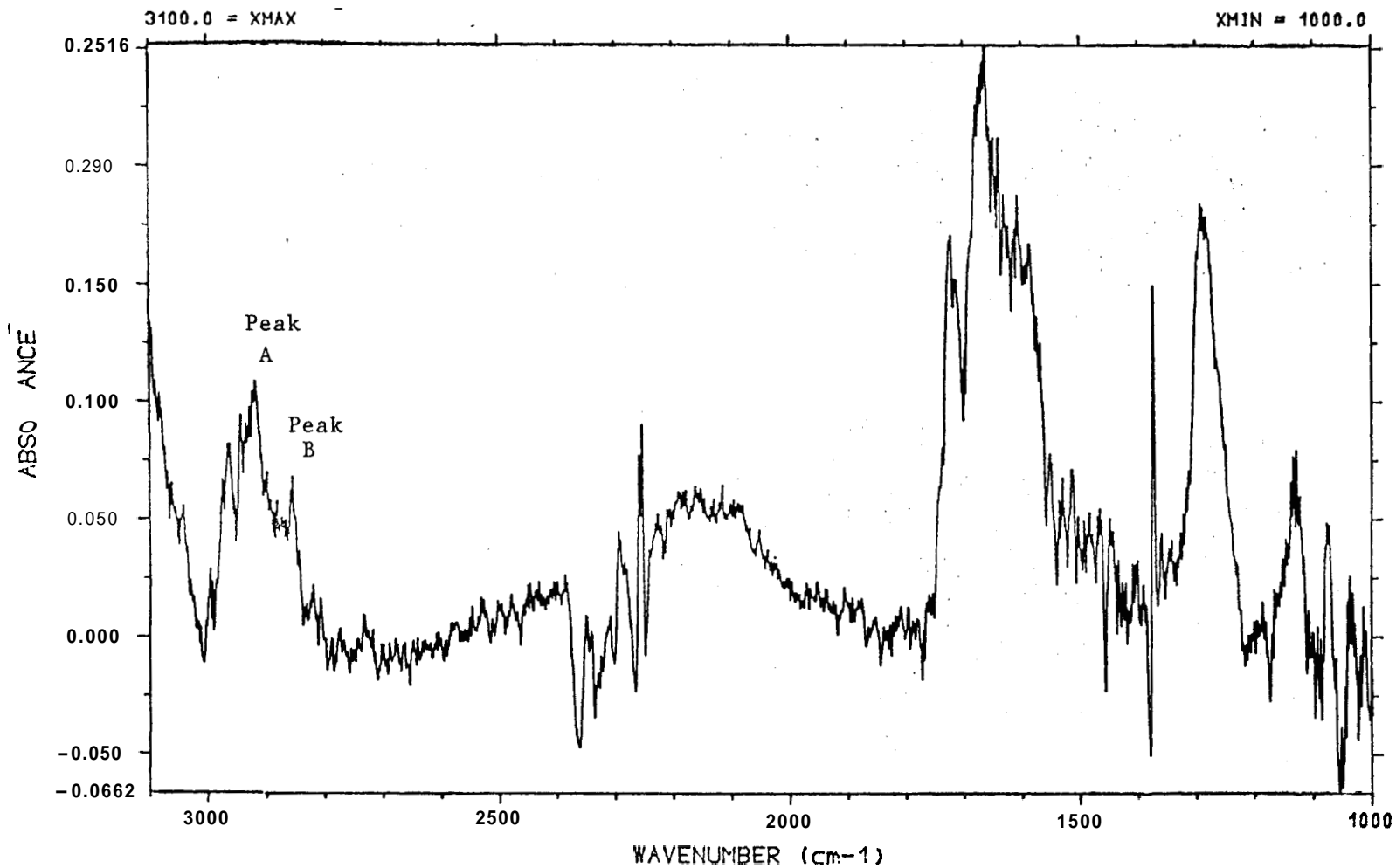


Figure 13. SAMPLE NAME : 1-ADAMANTANAMINE IN 75% ACETONITRILE AT PH 11  
SAMPLE FORM : FLOW-THRU CIRCLE CELL  
OPERATOR : ROSEANN BACA





To interpret the characteristics of an infrared spectrum, a correlation chart is used. The region from 4000-1400  $\text{cm}^{-1}$  is useful for the identification of various functional groups. This region shows absorption bands arising from stretching modes. Using this chart peak A and B may be attributed to the C-N stretch vibrational modes.<sup>35</sup>

#### Determination of pKa Values

In order to study the acid/base properties of 1-adamantanamine, the  $\text{pK}_a$  values for the drug were calculated using the net absorbance changes of peak A and B in varying solvents and pH. These values are listed in Tables 2, 3, 4, and 5.

The net absorbance changes of these peaks were then used to obtain an S-shaped curve of absorbance vs pH. Figure 14 illustrates the type of curve which is obtained. In the acidic range, high  $\text{H}^+$  concentration, there is a predominance of the HA form. While in the alkaline range, low  $\text{H}^+$  concentration, there is a predominance of the  $\text{A}^-$  form. Figures 15, 16, 17, 18, 19, 20, 21, and 22 illustrate the curves obtained.

Using these curves, the relative values for  $[\text{A}^-]$  and  $[\text{HA}]$  can be determined. The ratio of  $[\text{A}^-]$  and  $[\text{HA}]$  is then calculated using the following formula:<sup>36</sup>

$$\frac{[\text{A}^-]}{[\text{HA}]} = \frac{A - A_a}{A_b - A} \quad (1)$$

Typical values for A,  $A_a$ , and  $A_b$  are depicted in Figure 14.



Figure 2 - EXPERIMENTAL DATA OBTAINED FROM PEAKS A AND B IN AQUEOUS SOLUTIONS

	Net Absorbance		Log [A-]/[HA]	
	Peak A	Peak B	Peak A	Peak B
5	0.0044	0.0023	---	---
6	0.0049	0.0023	---	---
7	0.0053	0.0026	---	---
8	0.0061	0.0035	---	---
9	0.0098	0.0058	-1.39	-1.02
10	0.0282	0.0147	-0.65	-0.39
10.5	0.0436	0.0241	-0.36	0.07
11	0.0665	0.0380	-0.03	0.45
11.5	0.0763	0.0405	0.41	0.90
12	0.1261	0.0411	---	---
12.5	0.1300	0.0420	---	---
13	0.1319	0.0425	---	---



Figure 3 - EXPERIMENTAL DATA OBTAINED FROM PEAKS A AND B IN 25%  
ACETONITRILE SOLUTIONS

pH	Net Absorbance		Log [A <sup>-</sup> ]/[HA]	
	Peak A	Peak B	Peak A	Peak B
5	0.0116	0.0006	---	---
6	0.0118	0.0010	---	---
7	0.0116	0.0009	---	---
8	0.0123	0.0013	---	---
9	0.0123	0.0012	-1.00	-1.39
10	0.0133	0.0022	-0.69	-0.74
10.5	0.0150	0.0040	-0.38	-0.26
11	0.0159	0.0065	-0.12	0.14
11.5	0.0179	0.0076	0.24	0.62
12	0.0210	0.0096	---	---
12.5	0.0214	0.0097	---	---
13	0.0215	0.0097	---	---



Figure 4 - EXPERIMENTAL DATA OBTAINED FROM PEAKS A AND B IN  
50% ACETONITRILE SOLUTION

pH	Net Absorbance		Log [A-]/[HA]	
	Peak A	Peak B	Peak A	Peak B
5	0.0007	0.0038	---	---
6	0.0021	0.0034	---	---
7	0.0023	0.0034	---	---
8	0.0044	0.0080	---	---
9	0.0069	0.0100	-0.65	-0.23
10	0.0116	0.0155	-0.31	0.11
10.5	0.0147	0.0166	-0.98	0.37
11	0.0263	0.0196	1.03	0.63
11.5	0.0277	0.0198	1.40	0.92
12	0.0282	0.0216	---	---
12.5	0.0284	0.0220	---	---
13	0.0286	0.0222	---	---





Figure 5 - EXPERIMENTAL RESULTS OBTAINED FROM PEAKS A AND B IN  
75% ACETONITRILE SOLUTION

pH	Net Absorbance		Log [A-]/[HA]	
	Peak A	Peak B	Peak A	Peak B
5	0.0106	0.0042	---	---
6	0.0110	0.0032	---	---
7	0.0114	0.0056	---	---
8	0.0175	0.0097	---	---
9	0.0180	0.0137	-0.58	-0.54
10	0.0248	0.0187	-0.24	-0.20
10.5	0.0279	0.0217	-0.18	0.08
11	0.0456	0.0315	1.60	0.53
11.5	0.0464	0.0382	---	---
12	0.0464	0.0385	---	---
12.5	0.0464	0.0386	---	---
13	0.0464	0.0386	---	---



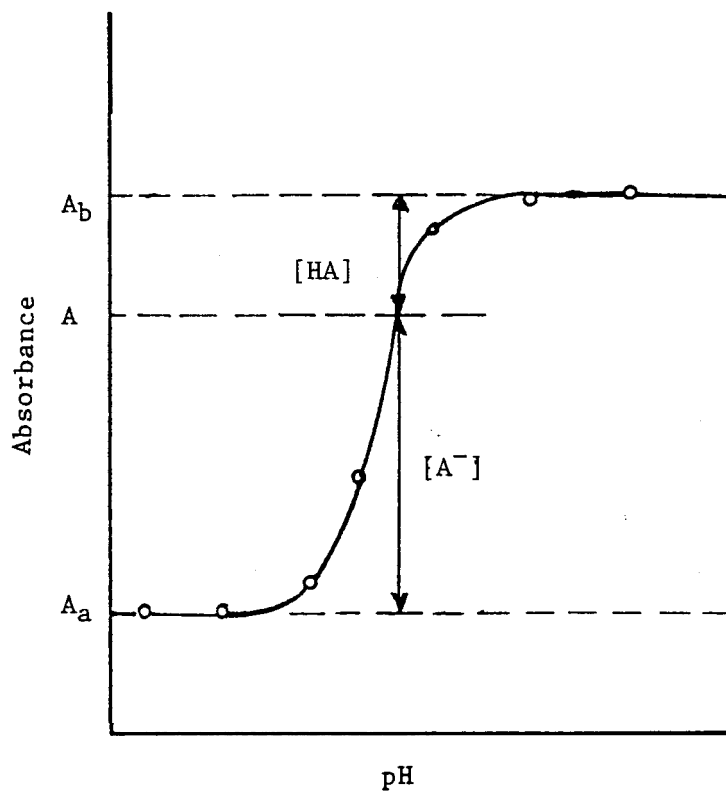


Figure 14. Typical plot of absorbance vs pH for a weak acid, HA. <sup>36</sup>



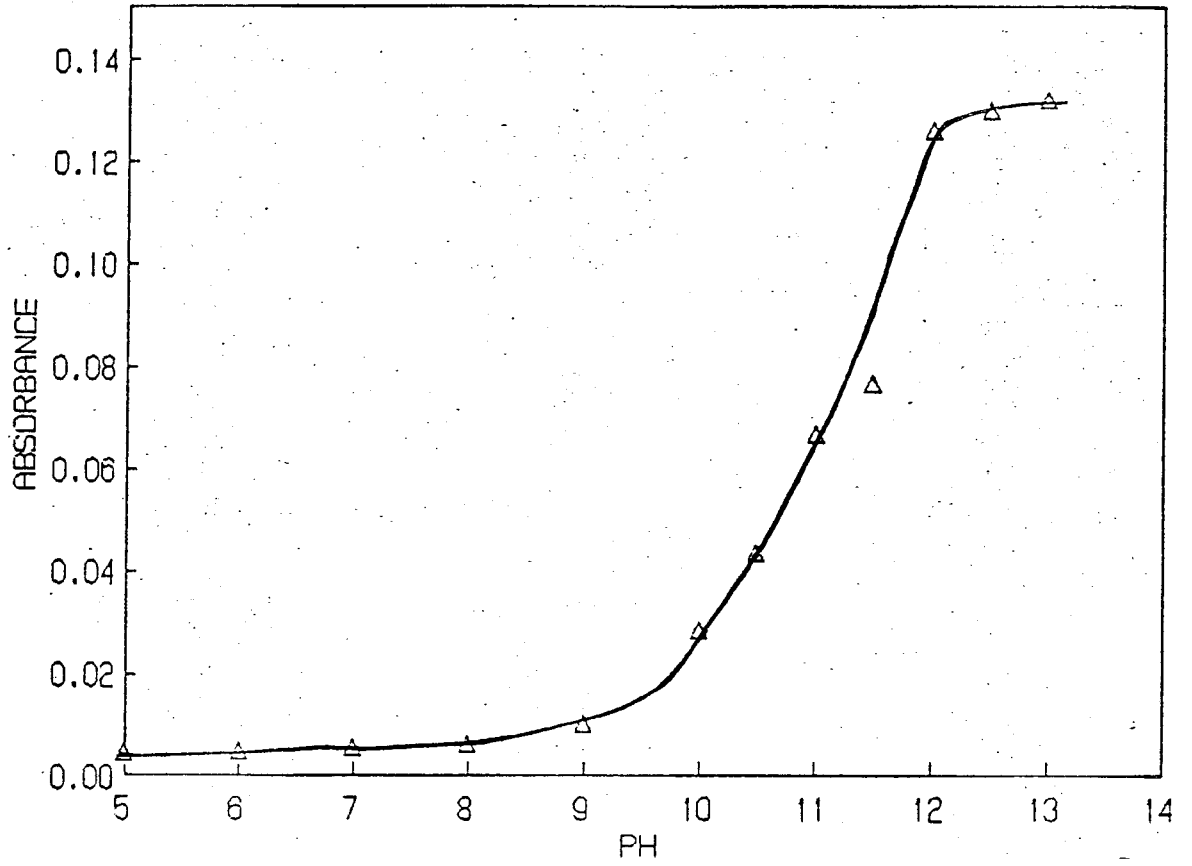


Figure 15. Absorbance Vs pH for Peak A in Water



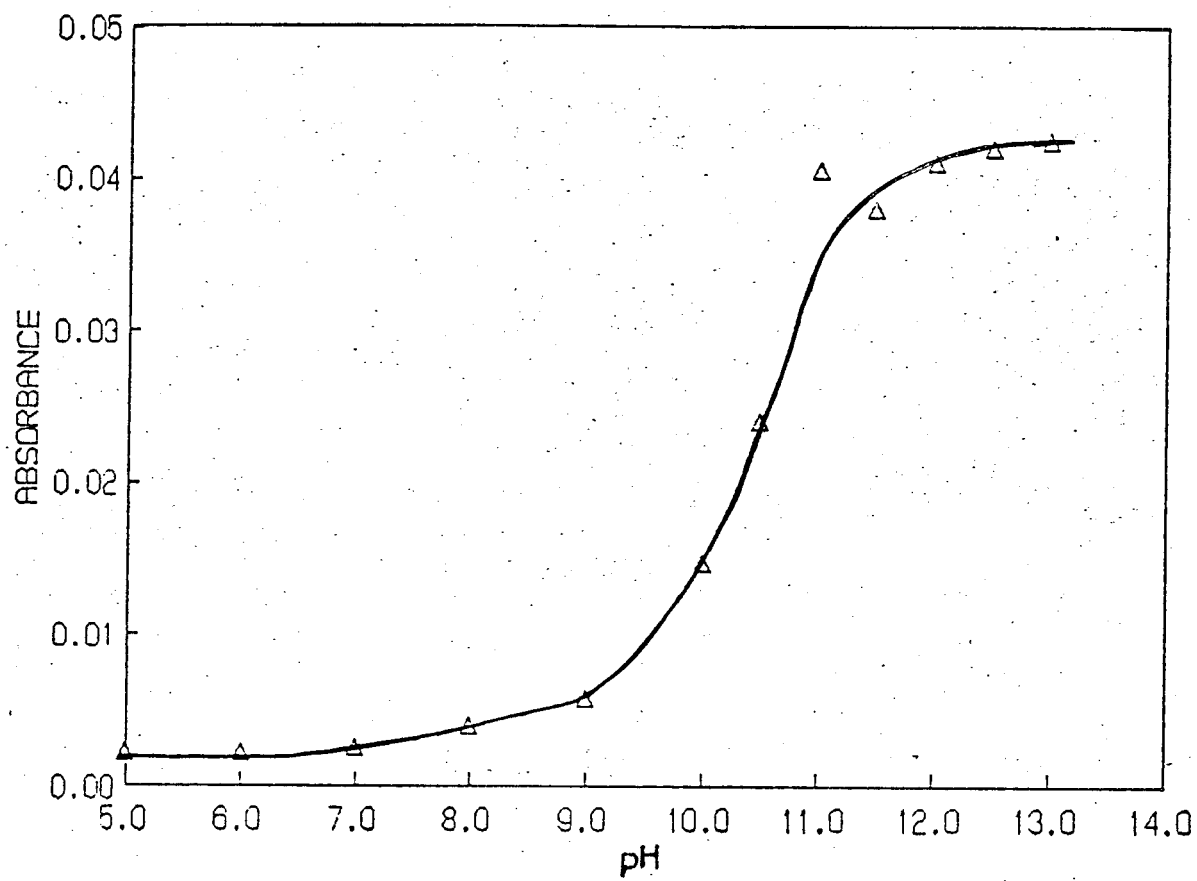


Figure 16. Absorbance Vs pH for Peak B in Water





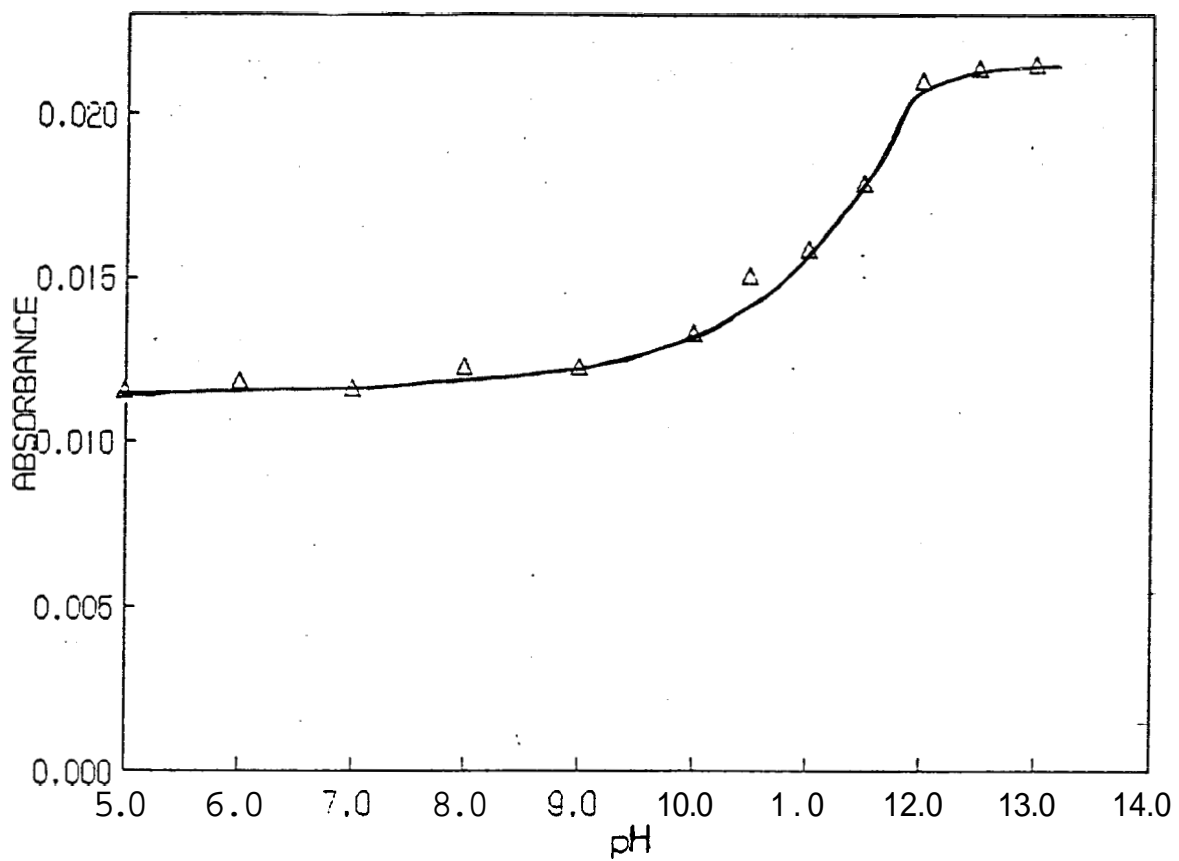


Figure 17. Absorbance Vs pH for peak A in 25% Acetonitrile



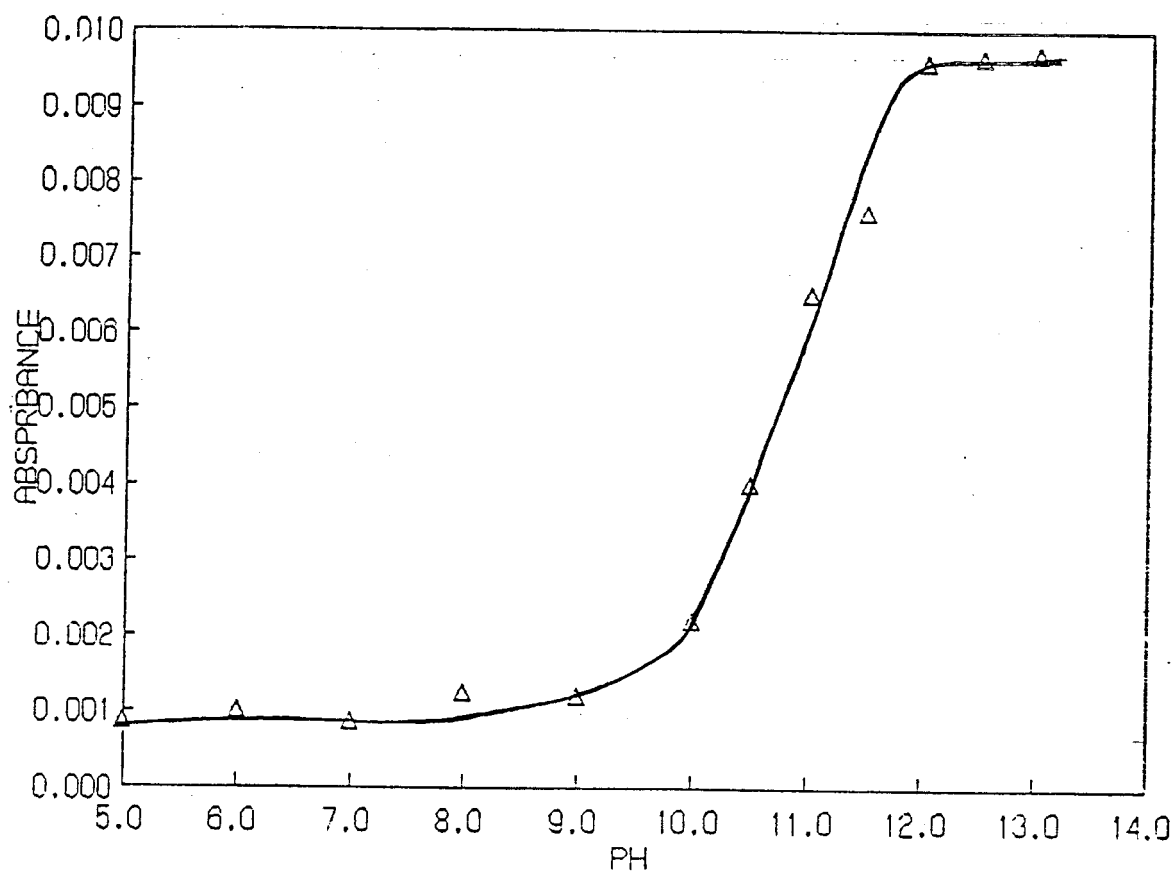


Figure 18. Absorbance Vs pH for Peak B in 25% Acetonitrile



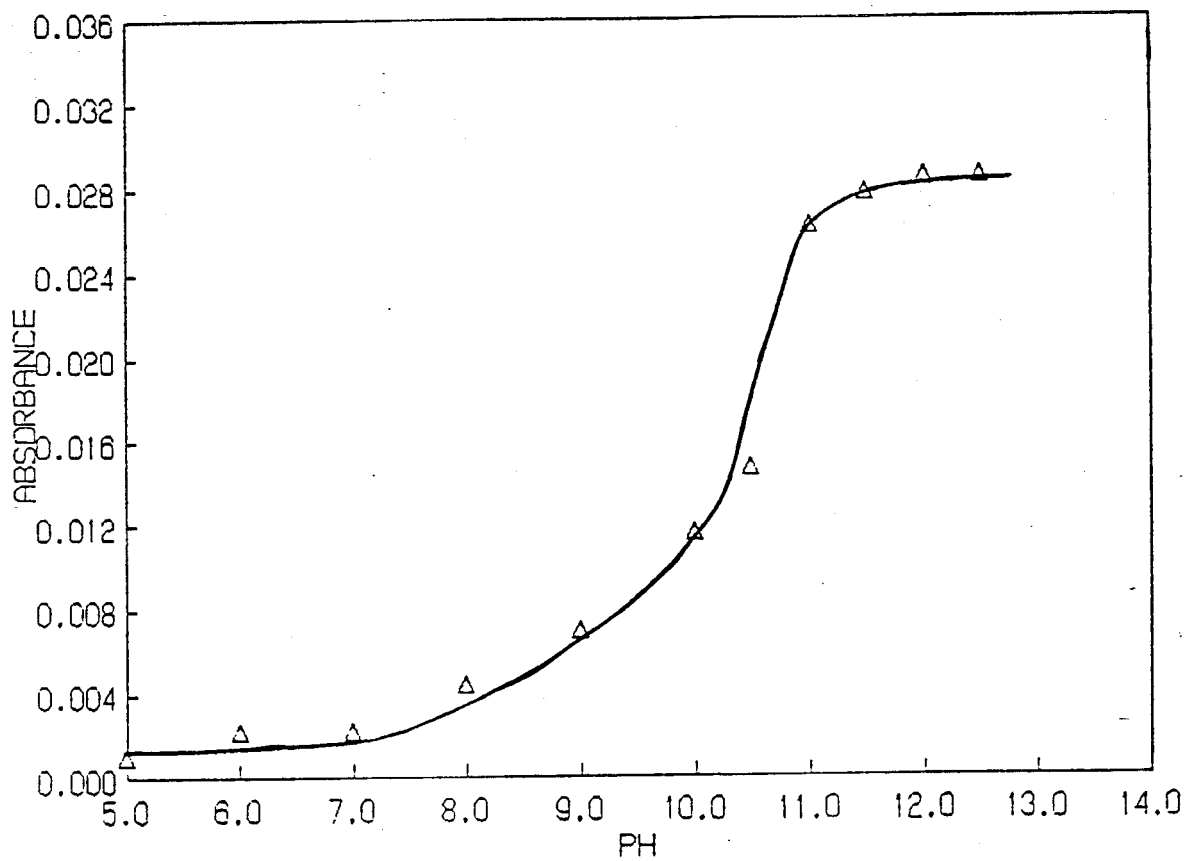


Figure-19. Absorbance Vs pH for Peak A in 50% Acetonitrile



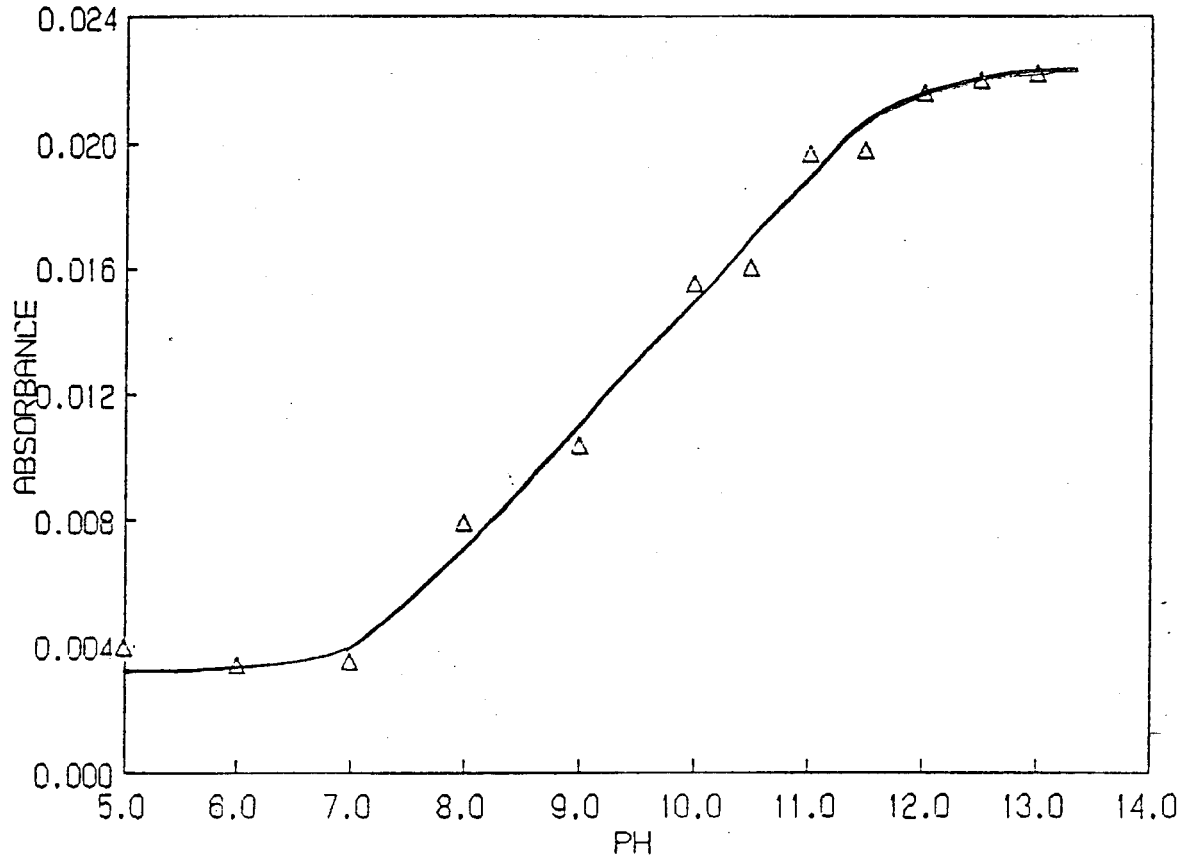


Figure 20. Absorbance Vs pH for Peak B in 50% Acetonitrile





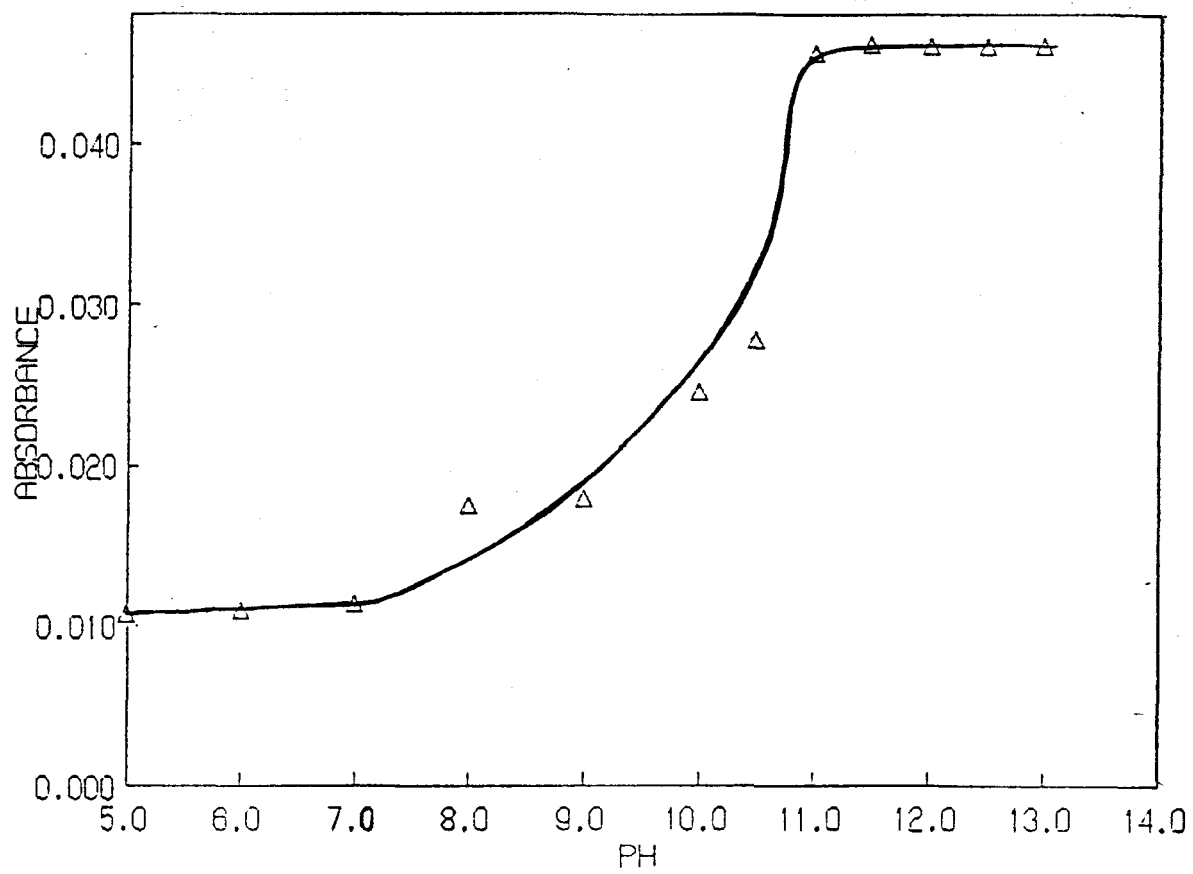


Figure 21. Absorbance Vs pH for Peak A in 75% Acetonitrile



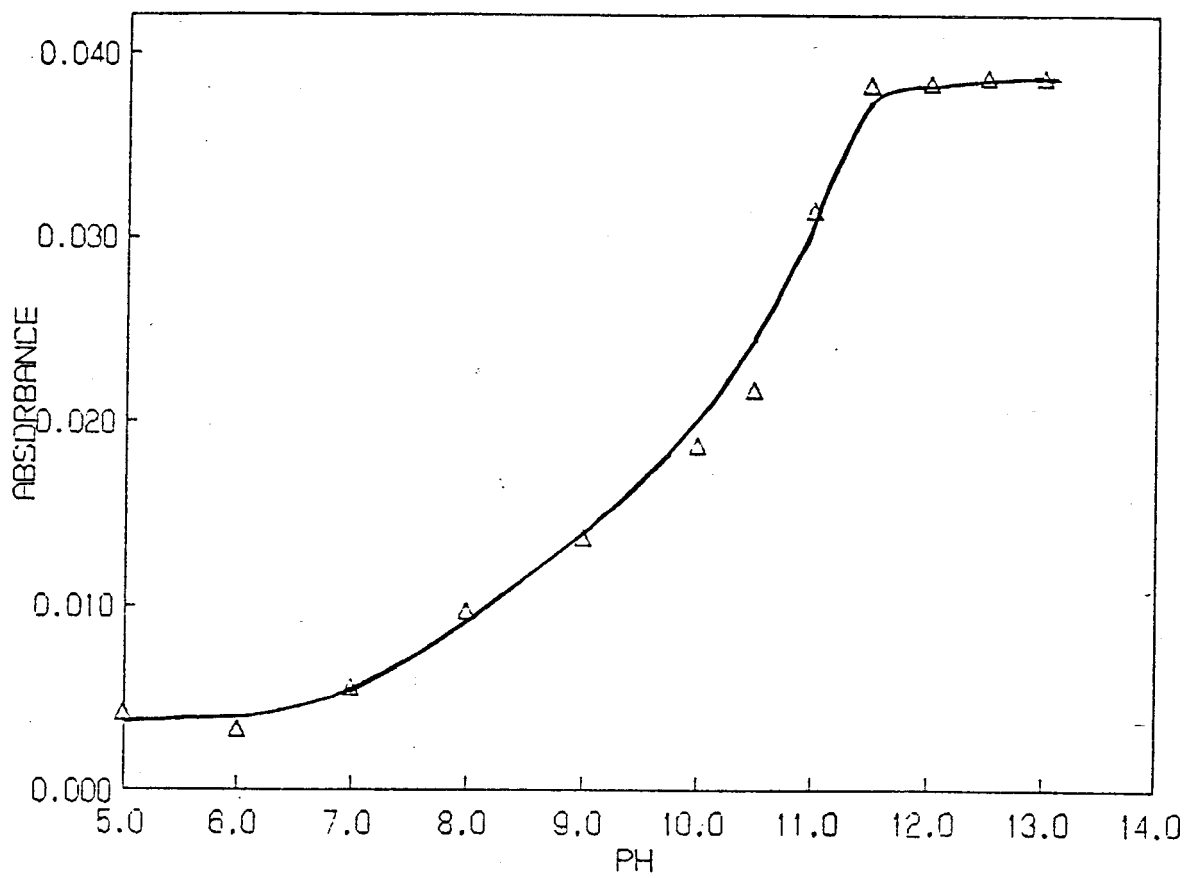


Figure 22. Absorbance Vs pH for Peak B in 75% Acetonitrile



The logarithm of this ratio is then calculated. These values are also listed in Tables 2, 3, 4, and 5.

These determinations can be calculated due to the dissociation of the compound. This dissociation may be represented by the formula,  $\text{HA} \rightleftharpoons \text{H}^+ + \text{A}^-$ . The equilibrium expression for such a dissociation can be written:<sup>36</sup>

$$K_a = \frac{[\text{H}^+][\text{A}^-]}{[\text{HA}]} \quad (2)$$

Taking the negative log of both sides of this equation and rearranging gives

$$\text{pH} = \text{p}K_a - \log \frac{[\text{HA}]}{[\text{A}^-]} \quad (3)$$

This can be rearranged in the slope-intercept form of a equation for a straight line to obtain:<sup>36</sup>

$$\log \frac{[\text{A}^-]}{[\text{HA}]} = \text{pH} - \text{p}K_a \quad (4)$$

Using this information as a basis for this experiment, the logarithm values of the ratios are obtained and plotted against the measured pH. Linear regression is used to calculate the best line fit, and from this graph the measured  $\text{p}K_a$  is determined by selecting the pH at which the line crosses the X axis. These graphs are illustrated in Figures 23, 24, 25, 26, 27, 28, 29, and 30.

The measured  $\text{p}K_a$  values can be obtained in this manner because of the slope-intercept equation of the line show in equation 3. In this equation  $y = \log [\text{A}^-]/[\text{HA}]$ ,  $m = 1$ , and  $b = -\text{p}K_a$ . So, when the log term is plotted vs pH, the slope is 1, the intercept is  $-\text{p}K_a$ , and the line crosses the pH axis at  $\text{pH} = \text{p}K_a$ . At this point  $[\text{A}^-] = [\text{HA}]$ , therefore, the log of the ratio of these terms is zero, making  $\text{pH} = \text{p}K_a$ .<sup>36</sup>



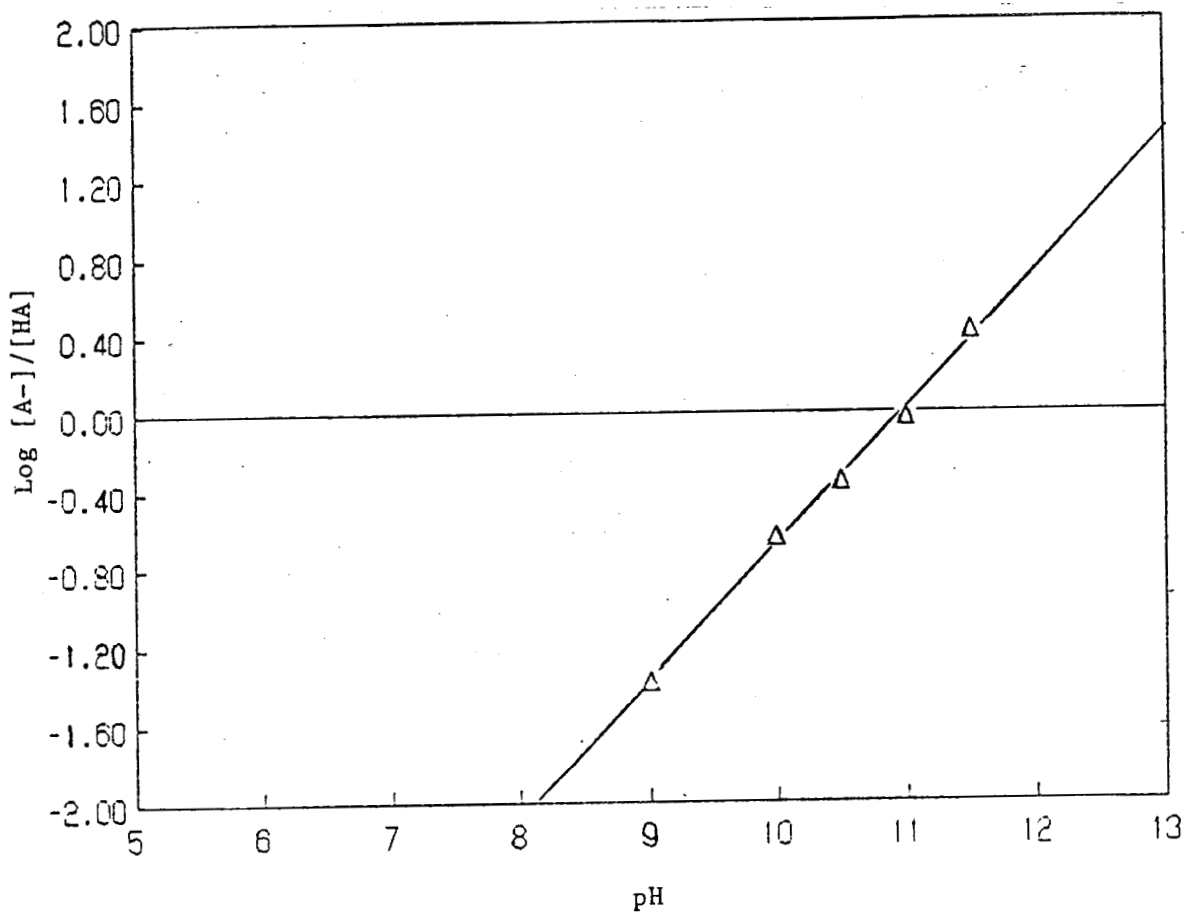


Figure 23.  $\text{Log } [A^-]/[HA]$  Vs pH for Peak A in Water





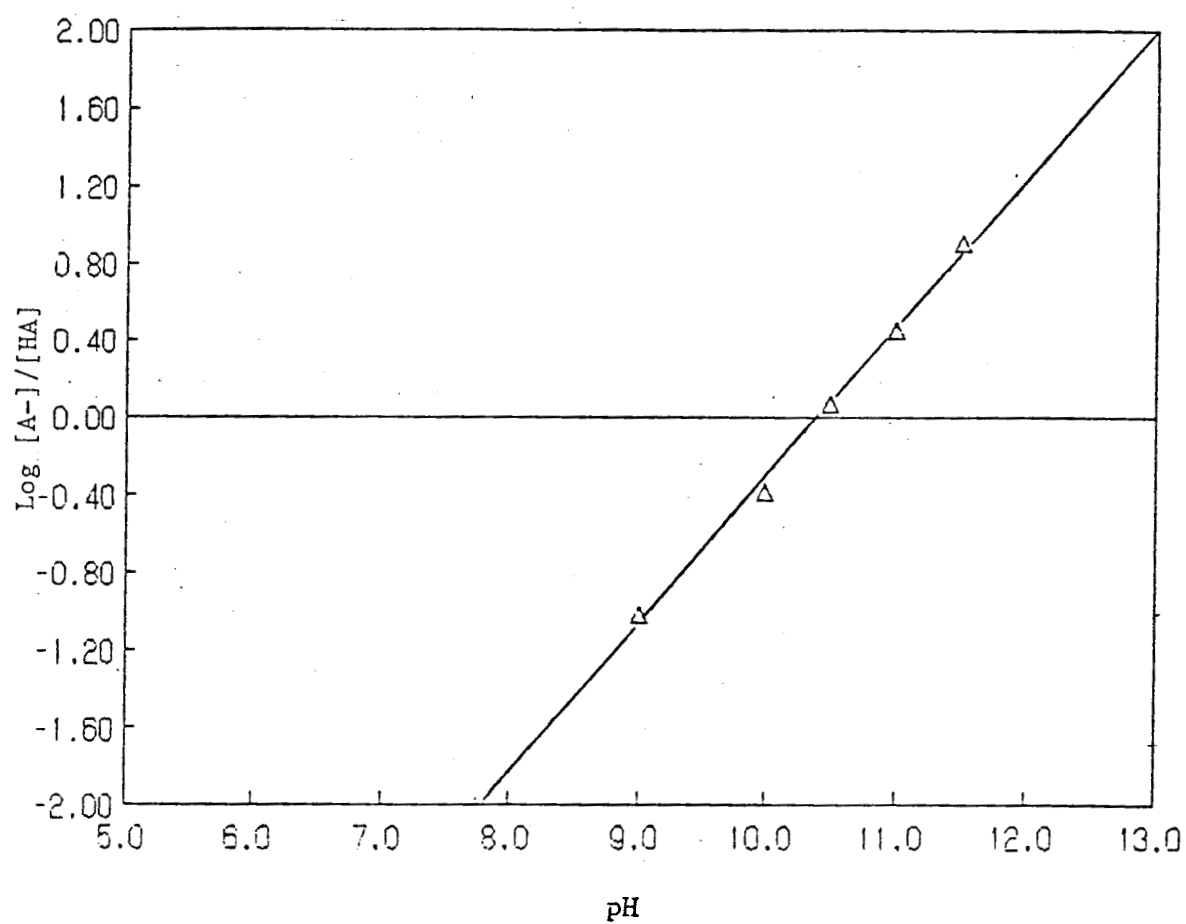


Figure 24.  $\text{Log } [A^-]/[HA]$  Vs pH for Peak B in Water



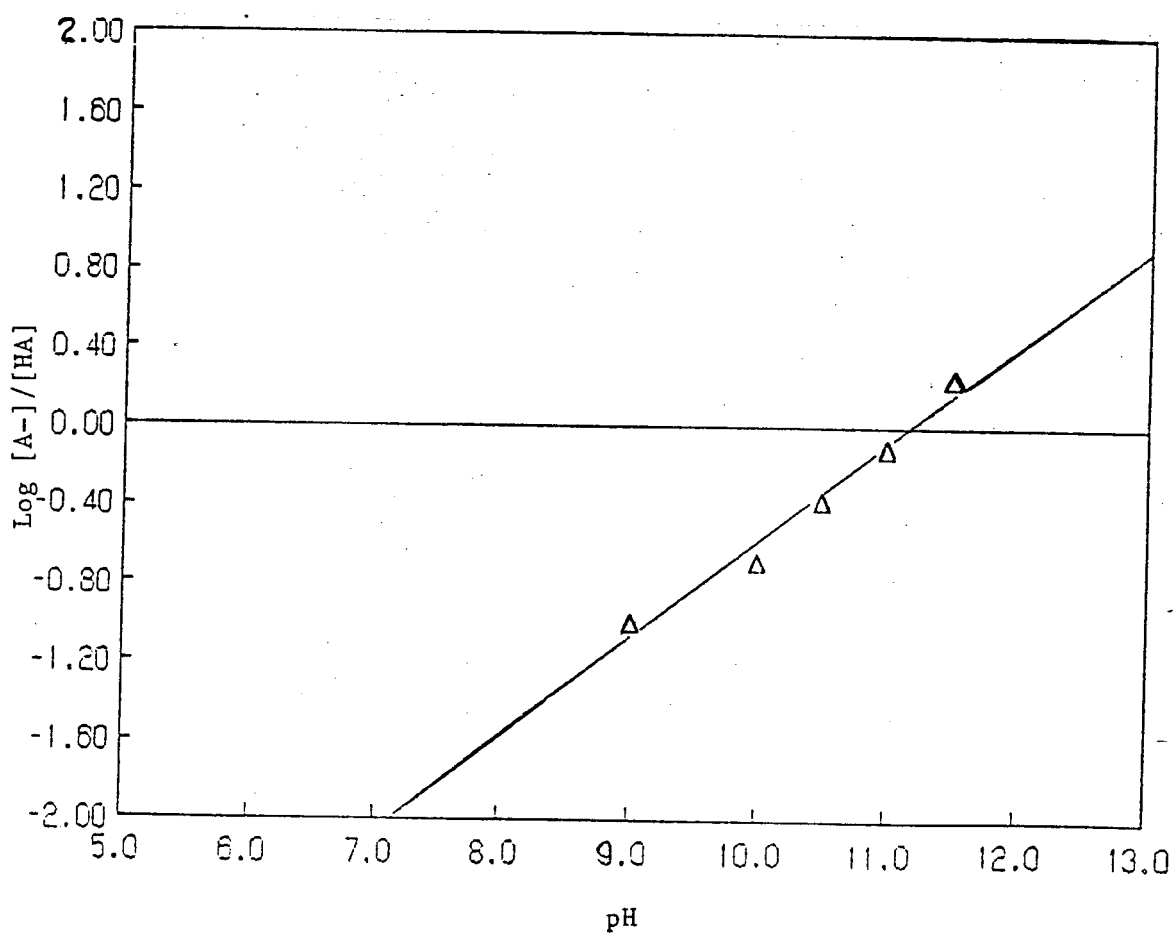


Figure 25. Log [A-]/[HA] Vs pH for Peak A in 25% Acetonitrile



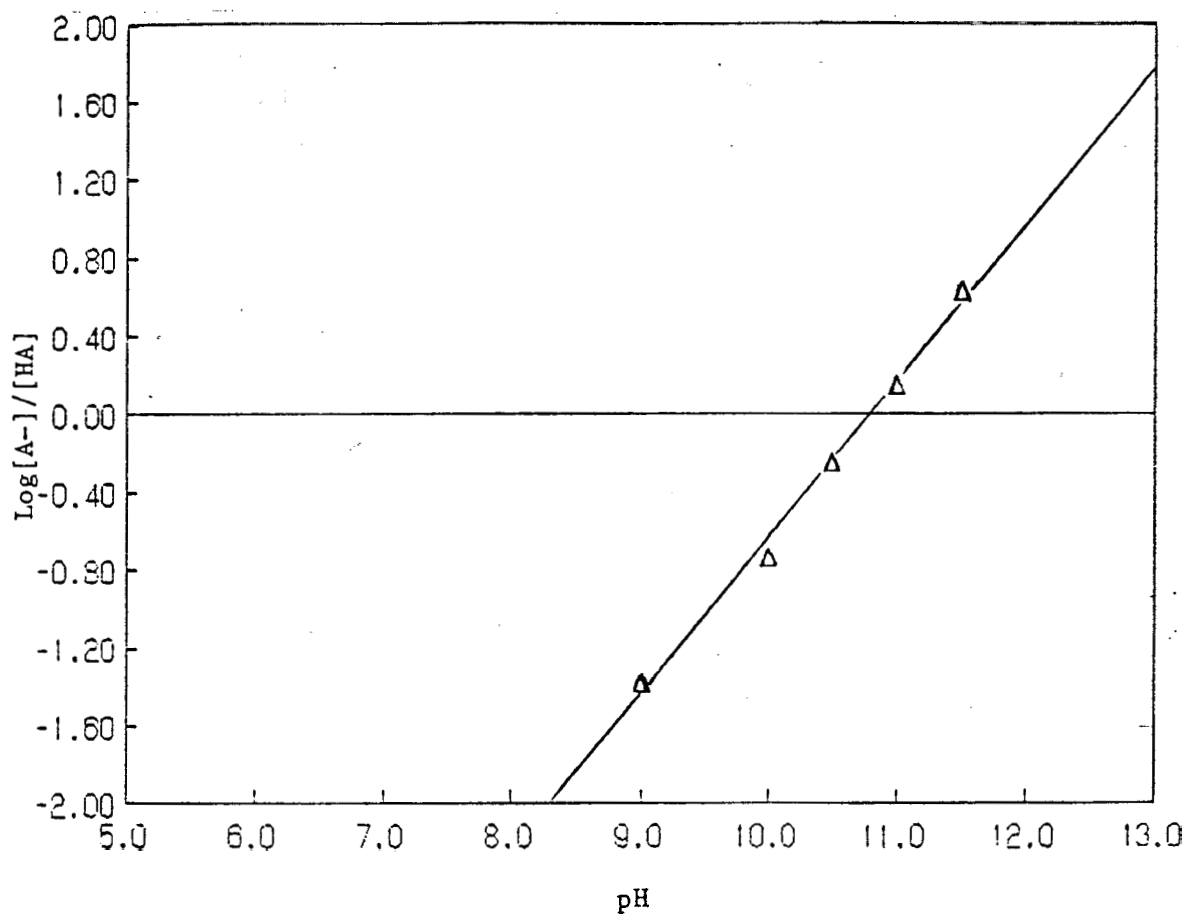


Figure 26. Log [A-]/[HA] Vs pH for Peak B in 25% Acetonitrile



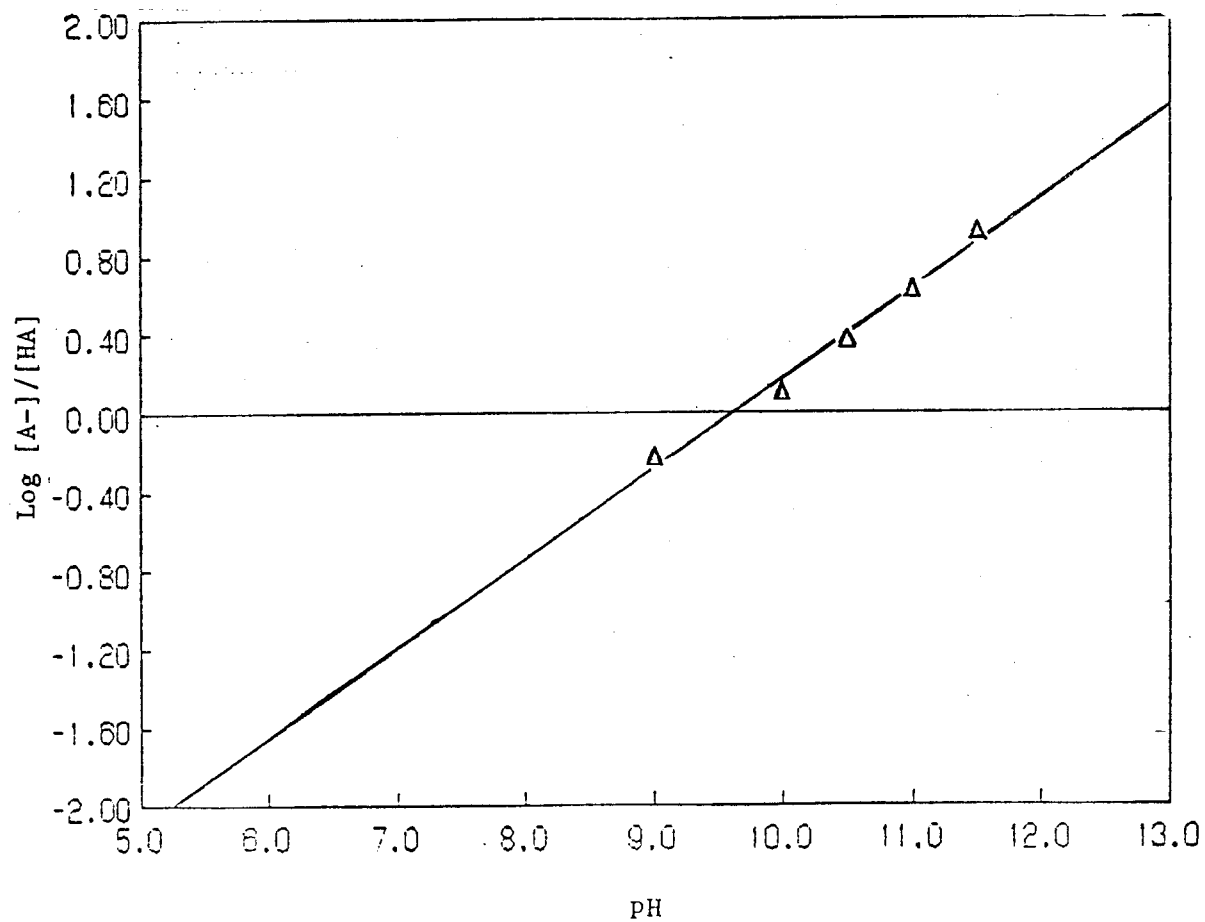


Figure 27.  $\text{Log } [A^-]/[HA]$  vs pH for Peak A in 50% Acetonitrile





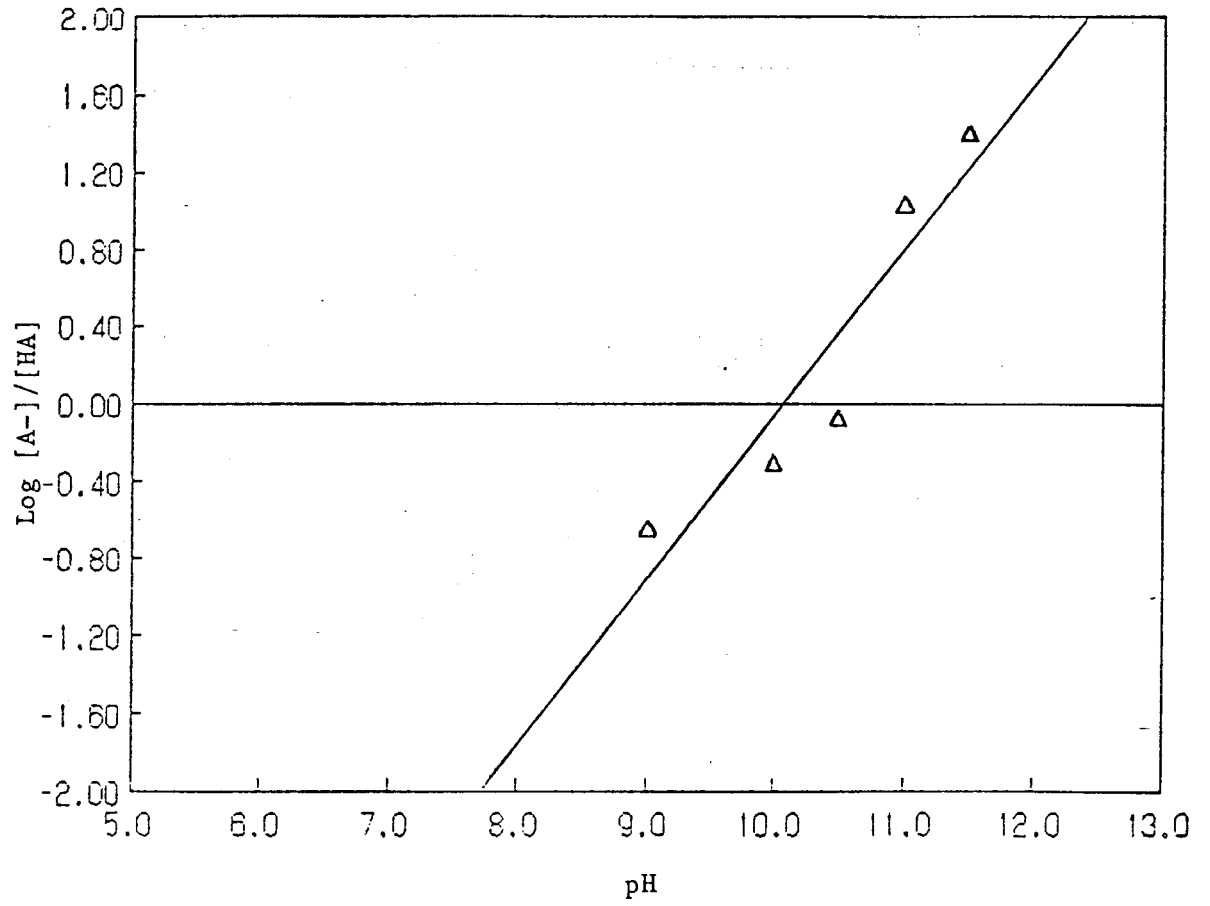


Figure-28.  $\text{Log } [A^-]/[HA]$  Vs pH for **Peak B** in 50% Acetonitrile



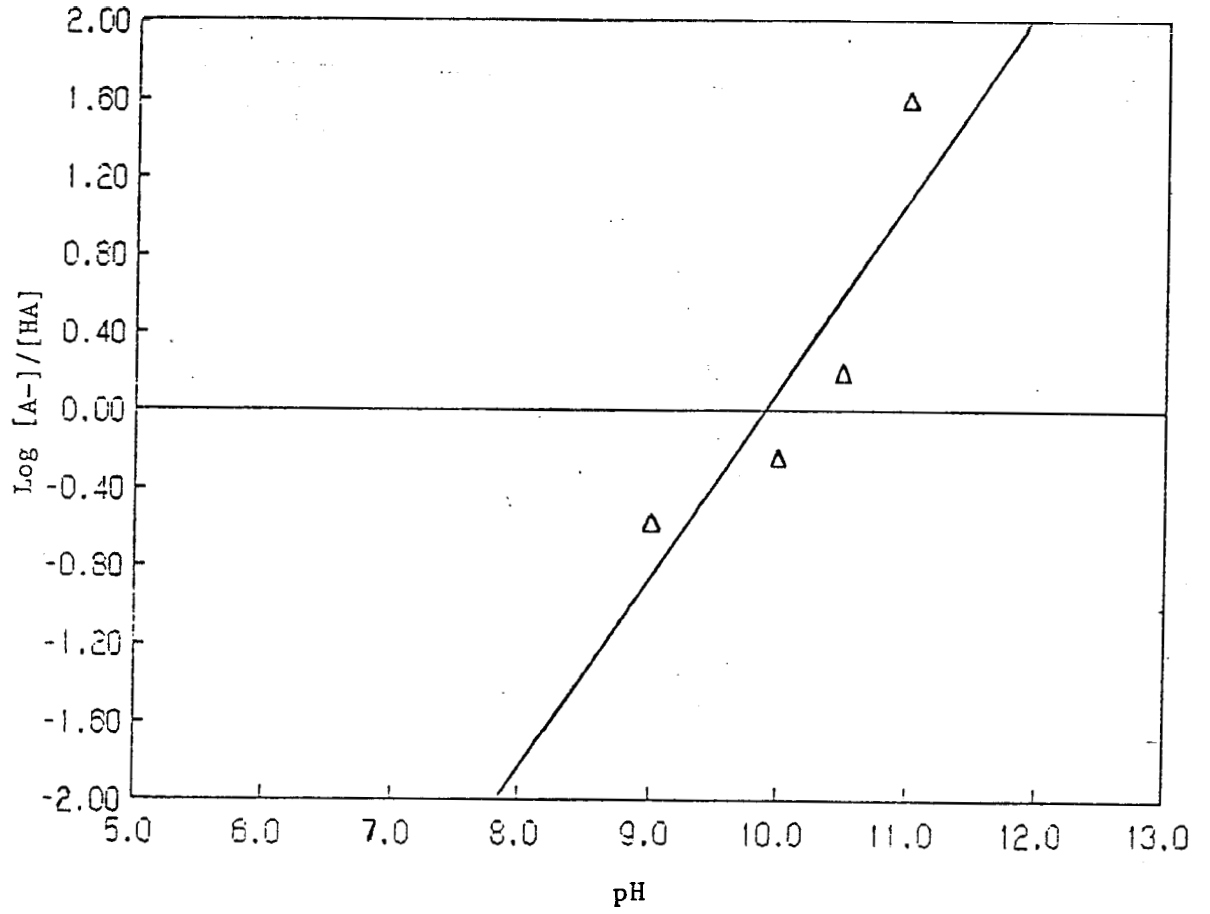


Figure 29.  $\text{Log } [A^-]/[HA]$  Vs pH for Peak A in 75% Acetonitrile



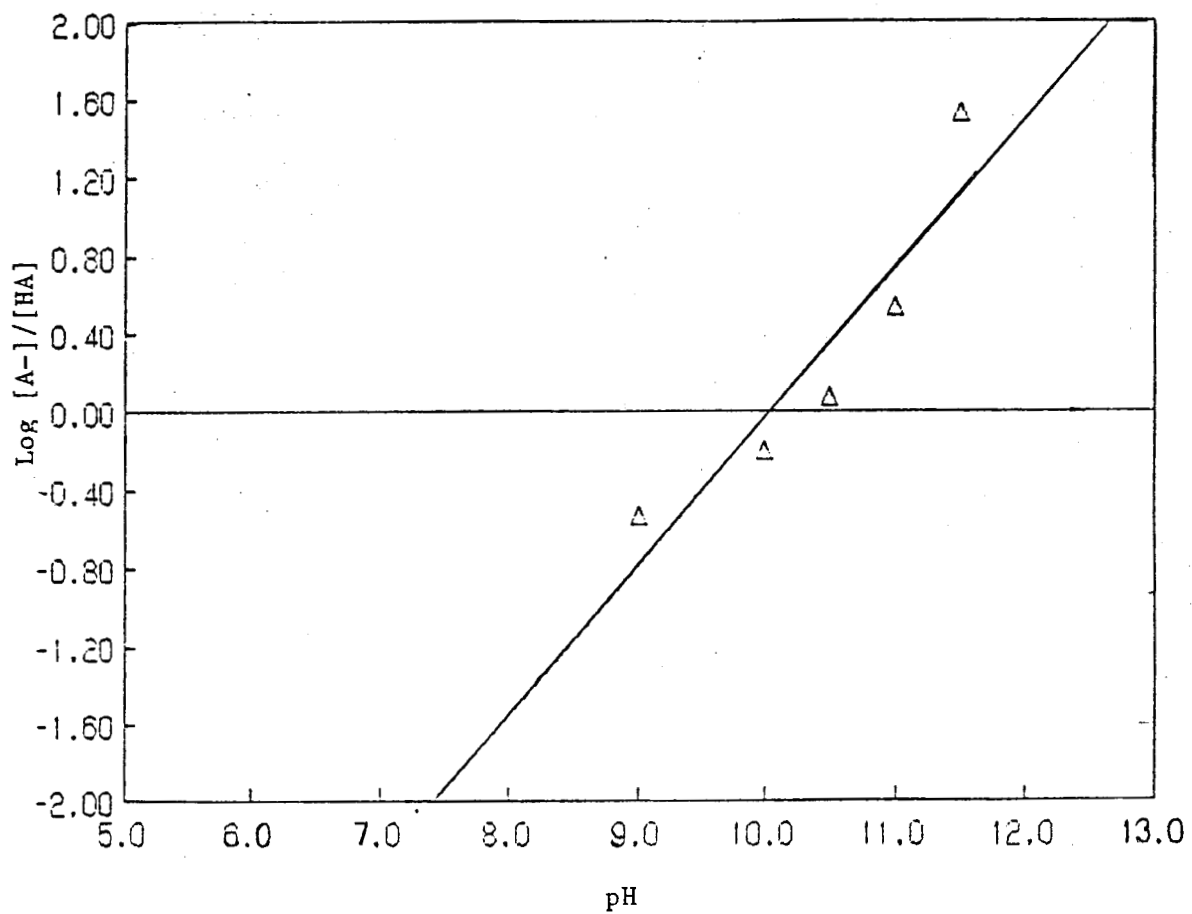


Figure 30.  $\text{Log } [A^-]/[HA]$  Vs pH for Peak B in 75% Acetonitrile



Once the measured  $pK_a$  or pH values ( $pH'$ ) are obtained, it is necessary to adjust these values. It is essential to do this because the hydrogen ion activity measured by the pH meter must be corrected because the electrode response is affected by solutions containing nonaqueous solvents. This is done by using a formula proposed by Mui and McBryde. The formula follows:

$$** = 10^{-pH'} / [H^+] \quad (5)$$

The symbol \*\* represents equilibrium constants established for mixed solvents.<sup>37</sup> These constants are 0.97 for 25% acetonitrile solutions, 1.22 for 50% acetonitrile solutions, and 2.42 for 75% acetonitrile solutions.<sup>38</sup>

Once the  $[H^+]$  is obtained using the formula for mixed solvents, the adjusted pH can be calculated. This is done by calculating the negative logarithm of the  $[H^+]$ . As stated earlier, the  $pH = pK_a$  at the pH intercept when  $\text{Log } [A^-]/[HA]$  is plotted vs pH, therefore, the values obtained are the adjusted  $pK_a$  values. These values are presented in Table 6.

% Acetonitrile	Adjusted $pK_a$	
	Peak A	Peak B
0	10.8	10.4
25	11.0	10.7
50	10.2	9.7
75	10.2	10.4

Table 6 - Adjusted  $pK_a$  values obtained from Peaks A and B in the various concentration of acetonitrile





## CHAPTER VI

### CONCLUSIONS

Experimentally, the  $pK_a$  value of **1-adamantanamine** in aqueous solution was determined. It appears that Fourier Transform Infrared Spectrometry can be used in this manner to obtain reproducible  $pK_a$  values. The  $pK_a$  values obtained for **1-adamantanamine** in water from peaks A and B are 10.8 and 10.4, respectively. The  $pK_a$  values derived from peaks A and B should have been identical, but were not because the  $pK_a$  value measured from peak B was less precise due to a lower absorbance intensity. These values are similar to the literature  $pK_a$  value for **1-adamantanamine** in water of 10.73.<sup>39</sup> As good agreement was obtained for aqueous solutions using this technique, solutions containing increasing concentrations of acetonitrile were measured.

The solvent acetonitrile was chosen because it is miscible in water, it has a very low basicity and no acidity, and the pH of the solutions can be determined with glass pH electrodes. As increasing concentrations of acetonitrile are used, the hydrophobicity of the solvent environment increases. This increase in hydrophobicity has been shown to influence the  $pK_a$  of several compounds including amino acids.<sup>3,37</sup> With these points in mind, it was felt that **this- $pK_a$**  study of mixed solvent solutions of varying hydrophobicity may be used to investigate potential changes in  $pK_a$  of **1-adamantanamine**.

In 25% acetonitrile, the adjusted  $pK_a$  values were determined to be 11.0 and 10.7. These  $pK_a$  values increased slightly above the values obtained in aqueous solutions. From this data, one could conclude in solutions of low hydrophobicity, the  $pK_a$  value will become greater.



But, this increase in  $pK_a$  did not continue. At 50% the adjusted  $pK_a$  of **1-adamantanamine** was calculated to be 10.2 and 9.7. One could surmise that the increasing hydrophobicity and the **amine** side chain of the drug are interacting to produce this  $pK_a$  decrease. This decrease in  $pK_a$  values did not continue. In 75% acetonitrile, the most hydrophobic solution, the  $pK_a$  values for **adamantanamine** were 10.2 and 10.4. Therefore, one can conclude that the  $pK_a$  will be maintained greater than 8 in a hydrophobic **environment**.

As was mentioned before, **1-adamantanamine** is a weak lysosomotropic base whose antiviral activity may be attributed to neutralization of lysosomal pH. This action lies in its ability to become protonated within the acid interior of the lysosomes. This results in the accumulation of the protonated **amine** in the lysosome. As this process occurs the lysosomal pH becomes buffered and the virus cannot penetrate the membrane.<sup>40</sup>

The concept described previously is known as trapping by protonation. It has been concluded that bases with higher  $pK_a$ 's are more sensitive to this effect. A base with a  $pK_a$  below 8 will not function in this manner.<sup>41</sup>

The  $pK_a$  of **1-adamantanamine** remains above 8. This indicates that it would be an effective lysosomotropic weak **base**. As the acetonitrile concentration increases, the conditions become more hydrophobic as would be the case at membrane surfaces. The adjusted  $pK_a$  values remain at approximately 10 with increasing acetonitrile content. Therefore, **1-adamantanamine** can be considered an effective lysosomotropic weak base.



In conclusion, Fourier Transform Infrared Spectrometry is useful in the determination of the effect of solvent and pH on **1-adamantanamine** solutions. This technique is useful because of Fellgett's advantage, the power and speed of the system's microcomputer, and the use of cylindrical internal reflectance.

Two problems did occur in this research project. The major problem concerns the cylindrical internal reflectance cell, the circle cell. This cell has a low throughput. Specifically, the percent of energy getting through the accessory without sample present is only 10-20% of the open beam throughput. This disadvantage is overcome somewhat by using the MCT detector, but accuracy problems still exist in determining spectra above  $3200\text{ cm}^{-1}$  in solutions containing low concentrations of moderately-absorptive samples.<sup>26</sup>

The second problem concerns the fact that only low concentrations of the drug could be used because of its low solubility. Only 0.013 M solutions could be made because the solutions became saturated.

Further studies using Fourier Transform Infrared Spectrometry in the determination of  $\text{pK}_a$  values should be pursued. Additional studies could be performed with **1-adamantanamine** in acetonitrile-KCl solutions. Also, other drugs such as anaesthetics and other antiviral agents can be tested. Furthermore, the technique used could be improved upon by utilizing a quantitative analysis software package.

Fourier Transform Infrared Spectrometry has been used to study polymers deposited as layers of 20-50 nm thickness upon the internal reflectance element.<sup>19</sup> It may be possible to apply this methodology to membrane studies. A membrane could be deposited on the surface of the



internal reflectance element. An aqueous or mixed solvent solution could be placed in the flow thru cell. It would then be possible to monitor the drug's  $pK_a$  values at various pH values using the technique developed in this work.





REFERENCES

1. Katzung, B.G., Basic and Clinical Pharmacology. Norwalk: Appleton and Lange, 1987.
2. Pouchert, C.J., The Aldrich Library of Infrared Spectra. Milwaukee: The Aldrich Chemical Company, 1981.
3. Windholtz, M., The Merck Index. New Jersey: Merck & Co., Inc., 1983.
4. Cassell, S., Edwards, J., and Brown, D.T., J. Virol., 1984, 52, 857-864.
5. Dolin, R., American Family Physician, 1979, 19, 127-130.
6. Wu, M.J., Ing, T.S., Soung, L.S., Davgirdas, J.T., Hano, J.E., and Gandhi, V.C., Clinical Nephrology, 1982, 17, 19-23.
7. Craig, C.R. and Stitzel, R.E., Modern Pharmacology. Boston: Little, Brown and Company, 1986.
8. Aviado, D.M., Pharmacologic Principles of Medical Practice. Baltimore: The Williams and Wilkins, 1972.
9. Kagan, B.M., Antimicrobial Therapy. Philadelphia: W.B.Saunders, Co., 1980.
10. Richmond, S. and Longson, M., The Practitioner, 1982, 226, 1711-1718.
11. Immunization Practices Advisory Committee, Morbidity and Mortality Weekly Report, 1986, 35, 317-326.
12. Council on Drugs, Journal of American Medical Association, 1967, 201, 114-115.
13. Koyama, A.H. and Uchida, T., Virol., 1984, 138, 332-335.
14. Skung, D.A. and West, D.M., Principles of Instrumental Analysis. Philadelphia: Saunders College, 1980.
15. Barrow, G.M., Physical Chemistry for the Life Sciences. New York: McGraw-Hill Book Company, 1981.
16. Silverstein, R.M., Bassler, G.C., and Morrill, T.C., Spectrometric Identification of Organic Compounds, New York: John Wiley and Sons, 1981.
17. Parker, F.S., Application of Infrared Spectrometry in Biochemistry, Biology and Medicine. New York: Plenum Press, 1971.
18. McDonald, R.S., Anal.Chem., 1982, 54, 1250-1275.



19. Griffiths, P.R. and deHaseth, J.A., Fourier Transform Infrared Spectrometry. New York: John Wiley and Sons, 1986.
20. Griffiths, P.R., Chemical Infrared Fourier Transform Spectroscopy. New York: John Wiley and Sons, 1975.
21. **IR/32** FTIR Spectrometer User's Manual, IBM Instrument, Inc., 1984.
22. Ferraro, J.R. and Basile, L.J., Fourier Transform Infrared Spectroscopy. New York: Academic Press, 1982.
23. Roth, M.S. and O'Donnell-Leach, D., Am. Lab., 1985, 17, 40-53.
24. Rein, A.J. and Morris, K.S., Am. Lab. , 1986, 18, 86-97.
25. Bartick, Dr., Am. Lab., 1984, 16, 56-62.
26. The Circle-Cylindrical Internal Reflection Accessory Instruction, IBM Instruments, Inc., 1984.
27. Hewitt, F.C., Morris, K.S., and Rein, A.J., Am. Lab., 1985, 17, 32-39.
28. Horlick, G. and Yuen, W.K., Anal. Chem., 1975, 47, 775A-780A.
29. Cooper, J.W., Anal Chem. 1978, 50, 801A-806A.
30. Wang, J.S., Rein, A.J., Wilks, D., and Wilks, Jr.P., Applied Spectro, 1984, 38, 32-35.
31. Orion Model SA 520 pH Meter Instruction Manual, Orion Research Incorporated, 1986.
32. Orion Electrode Pamphlet, Orion Research Incorporated
33. Fisher Scientific Catalog, Fisher Scientific Company, **1984-1985**.
34. Aldrich **Catalog/Handbook** of Fine Chemicals, Aldrich Chemical Company, 1984-1985.
35. Fessenden, R.J. and Fessenden, J.S., Organic Chemistry. Boston: PWS Publishers, 1982.
36. Day, R.A. and Underwood, A.L., Quantitative Analysis, Philadelphia: Prentice-Hall, 1986.
37. "The Effect of Solvent Hydrophobicity on the Acid-base Chemistry and Activity of Two Anti-Herpetic Drugs," Northeastern Ohio University College of Medicine, Ann F Stankewicz and Ken S Rosenthal.
38. Mui, K. and McBryde, W.A.E., Can. J. Chem, 1974, 52, 1821-1833.



39. Herzfeldt. C.D., Pharamazeutische Zeitung, 1980, 20, 606-614.
40. Seglen, P.O. and Gordon, R.P., Mol. Pharmacol., 1980, 18, 468-475.
41. Duve, C., Barsy, T., Poole, B., Trouer, A., Tulkens, P., and  
Van Hoof, F., Biochem Pharmacol., 1974, 23, 2495-2527.

